



## **Final report**

### **Project: Design of Advanced Joint Signal Processing Scheme for Multi-head Multi-track Recording Channels in BPMR and other High Areal Density Recording Systems**

**By**

**Asst. Prof. Dr. Lin Min Min Myint**

**Shinawatra University**

**April 2562**

# Contents

Title	Page
ABSTRACT .....	3
Chapter 1 Introduction .....	4
1.1 Background and Problem Statements .....	4
1.2 Project Objective .....	7
1.3 Project Scope .....	8
Chapter 2 Literature Review .....	9
2.1 Readback Channel Model .....	10
2.2 Realistic BPMR channel Model .....	11
2.3 Two-dimensional (2-D) Equalization .....	12
2.3.1 Symbol-based Trellis Design .....	15
2.3.2 Viterbi Algorithm for Detector .....	16
Chapter 3 Joint Signal Processing Scheme for Multi-head Multi-track Read Channel .....	19
3.1 Multi-track Joint Viterbi Detector for Multi-head Multi-track Read Channel .....	19
3.1.1 Four-head four-track Equalization and Detection .....	20
3.1.2 Multi-track 2-D Equalizer and 2-D GPR Target Approach .....	21
3.1.3 Multi-track Joint 2-D Detector .....	22
3.1.4 Numerical Evaluation .....	23
3.2 Reduced Complexity Multi-track Joint Viterbi Detector for MHMT Channel .....	25

3.2.1	Two MHMT channels (4H4T and 2H4T) .....	25
3.2.2	Multi-track Joint Equalizer and 2-D GPR target Design for Reduced Complexity Trellis	27
3.2.3	Multi-track Joint Detector with Reduced Complexity Trellis .....	27
3.2.4	Numerical Results.....	29
3.3	Noise Predictive Multi-track Joint Viterbi Detector .....	31
3.3.1	Noise Predictive Viterbi Detector .....	31
3.3.2	Noise Prediction Filter .....	32
3.3.3	Noise Prediction based on stored value on Surviving Path .....	33
3.3.4	Simulation Result and Discussion .....	35
3.4	Track Mis-registration Estimation .....	37
3.4.1	TMR Estimation Technique.....	39
3.4.2	Simulation Result .....	40
Chapter 4	Conclusion .....	42
Reference	.....	44
Appendix:	Publication List.....	48

## ABSTRACT

In future high areal density magnetic recording systems including Bit patterned media recording (BPMR), the prominent challenges to be addressed are two-dimensional (2-D) interference: Inter-symbol interference (ISI) and Inter-track interference (ITI) due to narrow the bit pitch and the track pitch, the media noise due to the size and position fluctuation, and track mis-registration (TMR) due to the misalignment of the head and the media. Without tackling them properly, they can severely impact on the performance of the read channel of magnetic recording systems. In the literature, read channels utilizing multi-head multi-track (MHMT) recording technology have been proposed to solve those problems because it can effectively tackle the 2-D interference and other impairments by processing multiple readback signals. However, most of proposed read channel system avoided full-fledged multi-track joint detection technique because of its impractically high complexity even though it is the most effective technique to combat 2-D interference in other areas such as image processing multi-input multi-output (MIMO) wireless communication.

Therefore, the aim of this research project is to design a novel advanced joint signal processing scheme with low complexity for multi-head multi-track recording system that can tackle the prominent problems in BPMR and other high density magnetic recording systems. In the project, various configurations of MHMT recording channel of BPMR systems are investigated and the trade-off between the performance and the complexity of the systems are made. Then, a low complexity multi-track joint detector is developed with the help of 2-D generalized partial response (GPR) equalization to recovery the recorded bits from the detecting tracks as well as from the sidetracks. Moreover, noise predictive Viterbi detectors for MHMT read channel of BPMR systems are studied and the project proposed a noise prediction technique based on the recorded noise information at the consecutive states along the surviving path leading to the current states. Finally, we proposed a TMR estimation technique with the terms of the coefficients of GPR target which is designed based on minimum mean squared error (MMSE) techniques.

# Chapter 1

## Introduction

### 1.1 Background and Problem Statements

In current Information age, people and their surrounding environments such as home, vehicles, pets, plants etc., are generating, processing and utilizing more and more data for their daily lives. Moreover, various emerging technologies such as Block Chain, IoT, Smart communities, Big Data etc. are data-intensive technologies and are integrating into many business areas. As a result of that, the demand for the data storage is growing in every hour, every day, every month. Nowadays, the two main data storage technologies are hard disk drive (HDD) which is based on magnetic recording technology, and solid-state drive (SSD) which based on integrated circuit technology. SSD is faster, more durable and need less energy; however, HDD is suitable for storing huge amount data because the cost per gigabyte (GB) or terabyte (TB) of HDD is still significantly lower than that of SSD. Therefore, HDD is still popular until now. In order to meet the rapid growing demand of the data storage, the research centers and the industries of HDDs are advancing to achieve higher areal density (storage capacity) with higher speed to meet the rapid growing demand of data storage,

In HDD or magnetic storage recording technology, bit patterned media recording (BPMR) technology, heat-assisted magnetic recording (HAMR) technology, microwave-assisted magnetic recording (MAMR) and two-dimensional magnetic recording (TDMR) have been proposed as the next generation ultra-high areal density. Recently, two leading HDD companies announced that they are launching over 10 TB HDDs which is more 2 Terabit per inch squared ( $2 \text{ Tb/in}^2$ ) with HAMR technology and MAMR technology respectively. In next decade, the areal density is planned to increase up to  $10 \text{ Tb/in}^2$  by combining two or three technologies. However, there are many challenges to be addressed in those technologies. Among them, the most prominent challenge is that its readback signal is corrupted by two-dimensional (2-D) interference: inter-symbol interference (ISI) and inter-track interference (ITI) because the spacing between adjacent islands at both along-track direction and cross-track direction are getting comparably narrower than the head's width [1],[2].

In a conventional magnetic recording channel, its readback signal is corrupted by ISI so that it can be equalized with a 1-D equalizer into a 1-D partial response (PR) target/generalized partial response (GPR) target and thereafter, a 1-D detector can be applied to recover the recorded bit. However, employing the 1-D detector is inappropriate for the 2-D interference channel of high areal density recording systems like BPMR because it cannot efficiently mitigate the ITI effect [3]. With a multi-head array or a single head with synchronized buffer memory, the multi-track joint, so called joint track, equalization techniques in conjunction with a pseudo 2-D or symbol-based detector are proposed in [3]-[5]; however, the aim of such detector is just to recover the recorded bit from a single track even though the equalizer needs to process multiple readback signals concurrently to shape the signal from the detecting track according to its 2-D GPR target. When compared to the conventional single-track 1-D equalization, this multi-track joint equalization technique does not significantly enrich the performance of detector in terms of Bit error rate (BER) because the minimum mean squared error (MMSE) criteria in this equalization does not help to enhance the desired a posteriori probability (APP) computation for estimating the recorded bit sequence in the 2-D detection technique [3],[4]. Alternatively, authors in [6] proposed a zero-ITI forcing multi-track joint equalization technique where ITI effects are completely eliminated from the readback signal of the detecting track, thereby using a 1-D detector. In conjunction with the multi-track joint equalizations, various techniques of using multiple 1-D detectors or simplified 2-D detectors with the help of iterative processing were investigated doing the trade-off between performance gain and complexity in [3], [7]-[9].

To tackle 2-D interference problem, multi-head multi-track (MHMT) recording technology using a multi-track joint detection technique has attracted many attentions recently [10]-[13] because processing the multiple readback signals from the same track or multiple adjacent tracks is viable to mitigate the ITI effectively in equalization and detection processes. Moreover, it can enhance the signal to noise ratio (SNR) and the signal to interference ratio (SIR) of the readback signal [11]. In [10], the researchers proved that such multi-track joint detection technique can achieve better performance by processing higher number of tracks jointly. Since its computational complexity can grow exponentially with the number of tracks/readback signals, it is infeasible to implement practically a multi-track joint detector for the MHMT recording technology. To address the penalty of high complexity challenge, we need to design

a multi-track joint detection technique with practicable complexity without paying the significant performance loss. In this project, it is important notice that the “multi-head multi-track (MHMT) recording technology” means that the system employs an array of multiple read sensors to generate the multiple readback signals from the same track and/or multiple adjacent tracks and the “multi-track joint detector” means the detector processing of the multiple signals/tracks together.

Besides the 2-D interference, the data recovery system of BPMPR experiences with the impacts of the media noise and track mis-registration (TMR). In fabrication process, lithographic techniques are unable to fabricate uniformly island arrays over large areas, and the resulting island arrays have a large variation in island geometry. The size and position variations of the islands generate the media noise in the readback signal [14], [15]. The TMR is happened due to the misalignment of the head from the track center while the data sequences are writing or reading on the media. At the readback channel side, the impact of TMR can provoke severer ITI effect since the track pitch is very narrow in BPMPR [16]. In MHMT channel, the output signals from 2-D equalizers are corrupted by the correlated/colored noise, and the performance of multi-track joint detector is not optimal due to it. Finally, these impairments can severely and cumulatively degrade the overall system’s performance; thus, they need to be considered carefully in the design of the read channel system for the high areal density recording systems.

In the literature, noise predictive detector is proposed to compensate the performance deficiency due to the colored noise [27-29]. Noise predictions for multi-track read channels are also studied in [30-31]. In a noise predictive detector, a linear noise predictor using finite impulse response (FIR) filter is employed to predict the current noise sample in terms of the most recent noise samples, and then, the predicted noise sample is used to correct the noise information in the branch metric calculation. In MHMT system, TMR information can be predicted based on the readback signals during the equalizer designing and the performance improvement of system with the help of the TMR prediction was shown. Exploiting the MHMT recording technology, equalizer processing multiple readback signals can handle the media noise and TMR impairments effectively while the detector processing the multiple readback signals from the difference adjacent tracks can tackle the 2-D interference [11]. Therefore, we

can enhance the performance degradation of MHMT recording system due to the reduced complexity multi-track joint detection with the predictive information of the residual and media noise and TMR impairments,

The research project aims to design a novel advanced joint signal processing scheme with low complexity for multi-head multi-track (MHMT) recording systems to combat the system impairments such as the 2-D interference, the media noise and TMR in BPMR as well as other high density magnetic recordings. Firstly, the project investigates various configurations of MHMT read channels of BPMR system doing trade-offs between performance and complexity for multi-track joint detectors including various reduced complexity methods for detector. For simplicity, we developed a readback channel model of the MHMT recording system for BPMR with using two heads to detect two tracks first and thereafter tried to detector more tracks. Then, we devised a multi-track joint detection technique with practicable low complexity level in conjunction with the help of 2-D joint GPR equalization for BPMR's MHMT read channels. The project also studied various noise predictive detectors for magnetic recording systems and proposed a noise prediction technique for multi-track joint detectors for MHMT reach channels that can addressed the colored noise problem as well as other noises such as mis-equalization and media noise. In the proposed technique, the noise prediction is done with the recorded noise samples along the surviving path without extending the trellis or computational complexity. Finally, a TMR estimation techniques is designed using the coefficients of 2-D GPR at equalizer designing process. Applying the estimated information and the noise prediction into the proposed detector, it is expected to improve the data recovery from the 2-D interference channel, but also in recovering the performance degradation.

## 1.2 Project Objective

1. To study multi-head multi-track (MHMT) read channels of BPMR system with inter-symbol interference (ISI) and inter-track interference (ITI) and the characteristics of media noise and Track-misregistration (TMR).



2. To study equalization and detection systems of MHMT read channels of BPMP system and other high areal density magnetic recording system.
3. To design and develop a novel multi-track joint detection technique with practicable complexity level for the MHMT recording system of BPMP and other high areal density recording systems
4. To design and develop a noise prediction technique for and a TMR estimation technique based on processing the multiple readback signals and they are intended to integrate into the proposed detection technique to improve the performance.
5. To evaluate the performance of proposed techniques comparing with the conventional multi-track joint detection technique and other techniques from the literature.

### **1.3 Project Scope**

The proposed techniques in this project are evaluated mostly for MHMT read channels of BPMP system because the main objective of the project is to tackle 2-D interference problem which is one the most dominant problems in all future high areal density recording systems.

## Chapter 2

### Literature Review

BPMR is one of the candidates for future ultrahigh density magnetic storage beyond 1 Tbit/in<sup>2</sup> [1]. In conventional storage, the aerial density is increased by reducing the bit cell; hence, fewer magnetic particles are contained, causing lower response and the instability of the magnetic field, known as “superparamagnetic effect”. In BPMR, each bit is recorded on an ordered array of highly uniform islands on a track of the magnetic film and each island includes a single magnetic grain to achieve high density and stability as shown in Fig. 1. Moreover, the non-magnetic boundaries between two adjacent islands can reduce the transition noise problem, which is one of the serious noises in the continuous magnetic media. In BPMR, the distances between islands in along-track and cross-track directions can be reduced to achieve the ultra-high aerial density. And as the read head senses the magnetization, the resulting readback signal is corrupted by a two-dimensional (2-D) interference that consists of inter-symbol interference (ISI) and inter-track interference (ITI) [2]-[8],[12], which is one of the main limitations for BPMR since it degrades the performance of the data recovery channel.

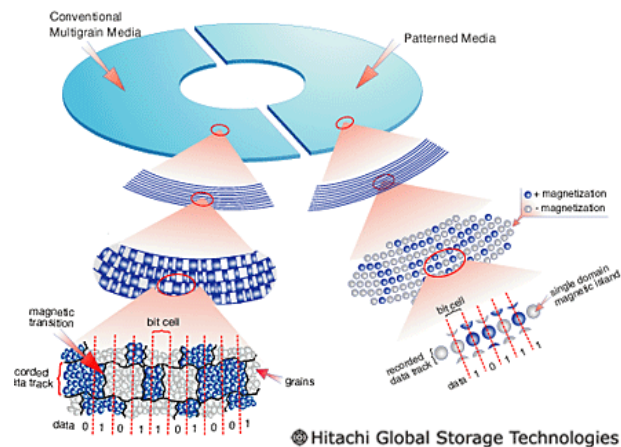


Fig.1. Comparison between conventional continuous domain recording and BPMR system.

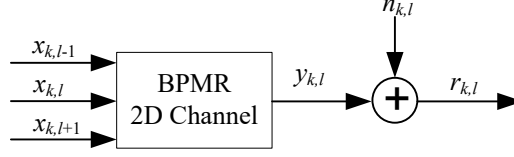


Fig. 2. The discrete-time channel model of typical BPMR recording system.

## 2.1 Readback Channel Model

A typical discrete-time channel model of BPMR recording system is illustrated in Fig. 2. In this model, the data bit at time  $k$  along the  $l^{\text{th}}$  track,  $x_{k,l}$ , is recorded on the BPMR media. The obtained BPMR readback signal  $r_{k,l}$  is expressed as

$$r_{k,l} = y_{k,l} + n_{k,l} = \sum_n \sum_m h_{n,m} x_{k-n,l-m} + n_{k,l} \quad (2)$$

where  $h_{n,m}$ 's are the 2D channel response coefficients and  $n_{k,l}$  is assumed to be additive white Gaussian noise (AWGN) [4]. Similar to [4], we assume that a read head detects the signal mainly from the track under it and some fractions from the above and below tracks as illustrated in Fig. 3. Without the TMR, a discrete-time 3x3 symmetric channel response matrix  $\mathbf{H}$  [4], [6], in the form of

$$\mathbf{H} = \begin{bmatrix} h_{k-1,l-1} & h_{k,l-1} & h_{k+1,l-1} \\ h_{k-1,l} & h_{k,l} & h_{k+1,l} \\ h_{k-1,l+1} & h_{k,l+1} & h_{k+1,l+1} \end{bmatrix}, \quad (3)$$

where  $h_{m,n}$ 's are the channel coefficients. The coefficients of the channel matrix in (2) and (3) can be generated by sampling the 2-D Gaussian pulse response at the integer multiples of the bit period and the track period [14]. The 2-D channel response coefficients  $h_{m,n}$  of BPMR system is generated by sampling the 2-D Gaussian pulse response at the integer multiples of the bit period  $T_x$  and the track pitch  $T_z$  i.e.,

$$h_{m,n} = A \exp \left\{ -\frac{1}{2} \left[ \left( \frac{nT_x}{cPW_x} \right)^2 + \left( \frac{mT_z}{cPW_z} \right)^2 \right] \right\}, \quad (4)$$

where  $A$  is the maximum amplitude of the pulse response.  $PW_x$  and  $PW_z$  are the location of the islands and the width of the pulse response at it half maximum ( $PW_{50}$ ) in the along-track and cross-track directions, and  $c = 1/2.3458$  is a constant [14].

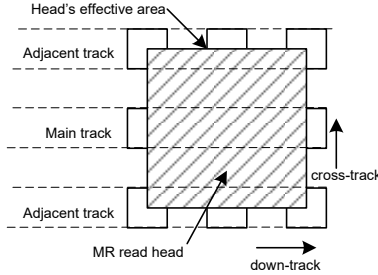


Fig. 3. The read head affective area over the 3x3 bit islands.

## 2.2 Realistic BPMR channel Model

Since the media noise is the prominent noise in BPMR system, it needs to consider the media noise in the channel model. To integrate the media noise, the pulse response is modified to include the island size and position fluctuation [16]. Therefore, the 2-D Gaussian pulse response with the media noise for the BPM media in this study is

$$P(x, z) = (A + \Delta_A) \exp \left\{ -\frac{1}{2} \left[ \left( \frac{x + \Delta_x}{c(PW_x + \Delta_{PW_x})} \right)^2 + \left( \frac{z + \Delta_z}{c(PW_z + \Delta_{PW_z})} \right)^2 \right] \right\} \quad (5)$$

where  $A$  is the amplitude of the pulse response,  $x, z$ ,  $\Delta_A$  is the amplitude fluctuation,  $\Delta_x$  and  $\Delta_y$  are the location fluctuation, and  $\Delta_{PW_x}$  and  $\Delta_{PW_z}$  are the  $PW_{50}$  fluctuations. The fluctuations of location and size are modeled as the Gaussian processes with the standard deviation which is defined as the percentage of the bit period.

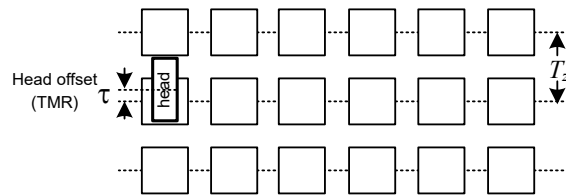


Fig. 4. TMR phenomenon in a BPMR system.

Moreover, TMR needs also to be considered in the channel model. Similar to [16], the channel response coefficients  $h_{m,n}$ 's are generated by sampling the pulse response of the isolated island from (5) at the integer multiples of the bit period and track pitch, i.e.,

$$h_{m,n} = P(-mT_x, -nT_z - \tau) \quad m, n \in -L, 0, L \quad (6)$$

where  $P(t_x, t_y)$  is the 2-D Gaussian pulse response,  $T_x$  and  $T_z$  are the bit period and the track pitch, and  $\tau$  is the head offset or the distance between the center of the head and the center of the island track as shown in Fig. 4. Without TMR, the value of  $\tau$  is zero, giving a symmetric channel matrix. With TMR, however, the channel matrix in (3), will be asymmetric. The sign of  $\tau$  is relative to the direction of the head offset. In here, we assume the sign is positive for the upward offset, but it is negative, otherwise. The TMR level is defined as

$$TMR(\%) = \frac{\tau}{T_z} \times 100. \quad (7)$$

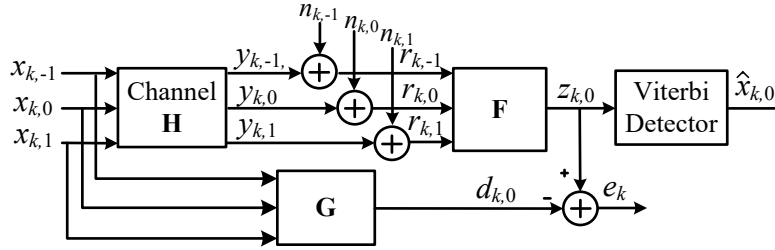


Fig. 5. Block diagram of 2-D Equalization in BPMP system.

## 2.3 Two-dimensional (2-D) Equalization

Since the readback channel is unknown in the magnetic recording system, therefore, the readback signal is usually equalized with the equalizer based on the desired target. In the conventional magnetic recording system, a 1-D partial response (PR) equalizer is applied with the fixed constant PR target. However, the performance of PR equalizer does not performance well with high areal density recording system. Alternatively, the equalizer with a generalized partial response (GPR) is proposed to use in the future magnetic technology like BPMP.

Figure 5 illustrates the model of the equalization for BPMR. In the equalization system, at the input of a 2-D equalizer  $\mathbf{F}$ , three adjacent readback signals  $\{r_{k,-1}\}$ ,  $\{r_{k,0}\}$  and  $\{r_{k,1}\}$  are required to generate a single output  $\{z_{k,0}\}$  since it includes the contribution of the adjacent tracks. Similarly, three input data sequences  $\{x_{k,-1}\}$ ,  $\{x_{k,0}\}$  and  $\{x_{k,1}\}$  are fed to the 2-D generalized partial response (GPR) target  $\mathbf{G}$  to give the desired output  $\{d_{k,0}\}$ . Define matrix  $\mathbf{F}$  with the size of  $3 \times (2N + 1)$  and the matrix  $\mathbf{G}$  with the size of  $3 \times 3$  as

$$\mathbf{F} = \begin{bmatrix} \mathbf{f}_{-1} \\ \mathbf{f}_0 \\ \mathbf{f}_1 \end{bmatrix} = \begin{bmatrix} f_{-N,-1} & \cdots & \cdots & \cdots & \cdots \\ f_{-N,0} & \cdots & \cdots & \cdots & \cdots \\ f_{-N,1} & \cdots & \cdots & \cdots & \cdots \end{bmatrix}, \quad (8)$$

$$\mathbf{G} = \begin{bmatrix} \mathbf{g}_{-1} \\ \mathbf{g}_0 \\ \mathbf{g}_1 \end{bmatrix} = \begin{bmatrix} g_{-1,-1} & g_{0,-1} & g_{1,-1} \\ g_{-1,0} & g_{0,0} & g_{1,0} \\ g_{-1,1} & g_{0,1} & g_{1,1} \end{bmatrix}. \quad (9)$$

In Fig. 5, the error signal  $e_k$  is the difference between the equalizer output signal  $z_{k,0}$  and the desired signal  $d_{k,0}$ . In order to design the equalizer coefficients using the minimum-mean squared error (MMSE) method, the mean-squared error (MSE) can be computed by

$$E\{(e_k)^2\} = E\{(z_{k,0} - d_{k,0})^2\} = E\{((r_{k,l} * f_{k,l}) - (x_{k,l} * g_{k,l}))^2\} \quad (10)$$

where  $E\{\cdot\}$  is the expectation and  $l \in \{-1, 0, 1\}$  and  $*$  is the convolution function. After expanding the righthand side, it becomes

$$E\{(e_k)^2\} = f_{k,l} * R_{k,l}^r * f_{k,l} - 2f_{k,l} * R_{k,l}^{rx} * g_{k,l} + g_{k,l} * R_{k,l}^x * g_{k,l} \quad (11)$$

where  $R_{k,l}^r = E\{r_{i,j}r_{i+k,j+l}\}$  and  $R_{k,l}^x = E\{x_{i,j}x_{i+k,j+l}\}$  are the auto-correlations of the readback signals and the recorded bits from all three tracks, respectively, and  $R_{k,l}^{rx} = E\{r_{i,j}x_{i+k,j+l}\}$  is the cross-correlation between the readback signal and the recorded bits. To compute the solution of MSE in (11), it is convenient to use the coefficient matrix and the target matrix in the vector forms [18] so that the matrices  $\mathbf{F}$  and  $\mathbf{G}$  are rearranged into the column vectors as  $\mathbf{f} = [\mathbf{f}_{-1} \ \mathbf{f}_0 \ \mathbf{f}_1]^T$  and  $\mathbf{g} = [\mathbf{g}_{-1} \ \mathbf{g}_0 \ \mathbf{g}_1]^T$ . Using those vectors, the MSE in (11) can be redefined as

$$E\{e(k)^2\} = \mathbf{f}^T \mathbf{R}_r \mathbf{f} - 2\mathbf{f}^T \mathbf{R}_{rx} \mathbf{g} + \mathbf{g}^T \mathbf{R}_x \mathbf{g} \quad (12)$$

where  $\mathbf{R}_r = [\mathbf{r}_k \mathbf{r}_k^T]$  is an auto-correlation matrix of  $R_{k,l}$  with the size of  $3(2N+1) \times 3(2N+1)$ ,  $\mathbf{R}_{rx} = [\mathbf{r}_k \mathbf{x}_k^T]$  is the cross-correlation of  $R_{k,l}^x$  with the size of  $3(2N+1) \times 9$  and  $\mathbf{R}_x = [\mathbf{x}_k \mathbf{x}_k^T]$  is an auto-correlation of  $R_{k,l}^x$  with the size of  $9 \times 9$ . The recorded bits vector  $\mathbf{x}_k$  and the readback signal vector  $\mathbf{r}_k$  are  $\mathbf{x}_k = [x_{k+1,1} \ x_{k,1} \ \dots \ x_{0,0} \ \dots \ x_{k,-1} \ x_{k-1,-1}]^T$  and  $\mathbf{r}_k = [r_{k+N,1} \ r_{k+N-1,1} \ \dots \ r_{0,0} \ \dots \ r_{k-N+1,1} \ r_{k-N,1}]^T$ . From [4], [6], to achieve the minimum MSE, the equalizer coefficients in  $\mathbf{f}$  for a given fixed target  $\mathbf{g}$ , can be obtained by

$$\mathbf{f} = \mathbf{R}_r^{-1} \mathbf{R}_{rx} \mathbf{g}. \quad (13)$$

## 5.6 Two-dimensional (2-D) or Symbol-based Detection

Like a communications channel, the magnetic recording system uses the optimum detection method for the data recovery system. The optimum detection method is based on the maximum-likelihood criterion for detecting sequence of symbols; also known as maximum-likelihood sequence detection (MLSD). It minimizes the probability of error for a received bit sequence [19]. An efficient algorithm for implementing MLSD is the Viterbi algorithm (VA). Burkhardt [20] proposed an optimal symbol-based Viterbi detector to apply in the high density data storage media of magnetic or optical. In the paper, the author predicted that, in the high areal density of future storage media, the read-back signal is corrupted by not only ISI and but also by ITI from the adjacent tracks when both linear density and track density are increased. To address this problem, a Viterbi detection method was proposed for the 2-D interference channels of the high density magnetic recording systems and in this method, the trellis is constructed by incorporating both ISI and ITI of the channel so that the detector can mitigate both of them. As a result of the high number of states and branches in the trellis, the decoding complexity is too high to implement in the real applications. However, we can consider as a baseline system for the single-track processing.

### 2.3.1 Symbol-based Trellis Design

In here, the 2-D interference channel is viewed as a 1-D equivalent interference channel by considering a non-binary symbol data or a column-wise recorded data bits from the adjacent tracks together. Since the input to the system is a symbol sequence, the trellis in here is constructed based on the non-binary symbol. Note that we explain the detector on the read-back channel of the BPMP system because we focus only in the BPM system in this work.

In the case of the 2-D BPMP channels, the read-back signal includes the contribution of the bit islands from the main track (the reading track) together with the interference from the bit islands on the two adjacent tracks and as illustrated in Fig. 3. Therefore, the read-back signal from the  $k^{\text{th}}$  recorded bit island at the  $l^{\text{th}}$  track,  $r_{k,l}$  is modeled as

$$r_{k,l} = \sum_{m=-1}^1 \sum_{n=-1}^1 h_{m,n} x_{k+m,l+n} + n_{k,l} = y_{k,l} + n_{k,l} \quad (14)$$

where  $h_{m,n}$  is the channel coefficients of a 2-D channel,  $x_{k,l}$  is the recorded bit on the island, and  $y_{k,l}$  is the noiseless read-back signal, and  $n_{k,l}$  is a AWGN noise. From (14) the BPMP channel has three input sequences, represents the recording data to the three adjacent tracks  $\{-1, l, l+1\}$  but it outputs a single read-back signal from the  $l^{\text{th}}$  track. Therefore, for the input side, the triplet of bits or a triplet bits  $(x_{k,l-1}, x_{k,l}, x_{k,l+1})$  from the three adjacent tracks at time  $k$  are considered together as a symbol vector  $\mathbf{x}_k = [x_{k,l-1}, x_{k,l}, x_{k,l+1}]^T$ . Since the recorded data sequences for all tracks are the binary data with  $\{-1, 1\}$ , the symbol  $\mathbf{x}_k$  has  $2^3 = 8$  alphabets.

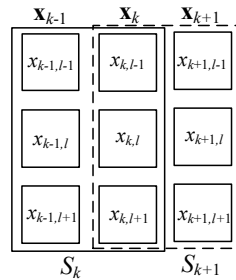


Fig. 6. Current state  $S_k$  (bold line) and next state  $S_{k+1}$  (dashed line)



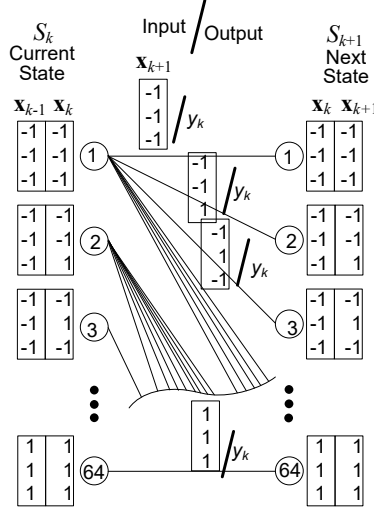


Fig. 7. Non-binary symbols state transition diagram of the 2-D interference BPM channel

Considering, a BPMR discrete domain of 2-D channel matrix from (3) or a 2-D GPR target matrix from (6), the 3x3 channel matrix can be considered as a row vector with the two symbol-based ISI and each symbol-based ISI is a column vector, including the ISI and two ITI. we can build a symbol-based trellis structure for the detector. In the trellis, the current state  $S_k$  is defined with the two symbols:  $\mathbf{x}_k$  and  $\mathbf{x}_{k-1}$  and the next state  $S_{k+1}$  is defined with the two symbols:  $\mathbf{x}_{k+1}$  and  $\mathbf{x}_k$  as illustrated in Fig. 6. Since each symbol  $\mathbf{x}_k$  has 8 possible outcomes, there are 64 possible states at each time  $k$  in the trellis and each state has 8 outgoing branches, each branch is related to one of the possible input symbols. According to the Markov process, the transition from the current state  $S_k$  to the next state  $S_{k+1}$  at time  $k+1$  depends on the current input and the current state. A state transition diagram for the symbol-based trellis is shown in Fig. 7. According to this trellis, there are  $64 \times 8 = 512$  branches in each transition. Therefore, the complexity of trellis might be too high to employ in practical application.

### 2.3.2 Viterbi Algorithm for Detector

The maximum likelihood sequence detection (MLSD), in particular Viterbi algorithm can be applied on the above trellis to recover the recorded input data from the BPMR media. The detection algorithm is considered based on the symbol input data and the symbol-based trellis; hence, the detector produces the estimated symbol sequence which is composed of triple bits.

However, the goal of the detector is to recover the recorded data on the main track so that the detector generates only the estimated bit sequence  $\{x_{k,l}\}$  from the main track.

After receiving the length  $N$  of the read back signal  $r_{k,l}$  from the main track, the MLSD detector selects the estimated input symbol sequence  $\hat{\mathbf{X}} = \{\hat{\mathbf{x}}_1, \dots, \hat{\mathbf{x}}_N\}$  by maximizing a likelihood function which is defined as

$$\hat{\mathbf{X}} = \arg \max_{\mathbf{X}} p(\mathbf{r}|\mathbf{X}). \quad (15)$$

In (11),  $p(\mathbf{r}|\mathbf{X})$  is the conditional probability density function (pdf),  $\mathbf{r} = \{r_1, r_2, \dots, r_N\}$  is the read-back signal sequence from the main track at the input of the detector and  $\mathbf{X} = \{\mathbf{x}_1, \dots, \mathbf{x}_N\}$  is the input symbol sequence. According to the trellis from Fig. 6, the input symbol sequence  $\mathbf{X}$  has the one-to-one relationship with a sequence of the state transitions  $\xi = \{\xi_1, \dots, \xi_N\}$ , a state transition  $\xi_k$  is defined as the transition of the current state  $S_k \equiv (\mathbf{x}_k, \mathbf{x}_{k-1})$  at time  $k$  and the next state  $S_{k+1} \equiv (\mathbf{x}_{k+1}, \mathbf{x}_k)$  at time  $k+1$ . To estimate the input symbol sequence, the detector estimate the state transition sequence by maximizing the likelihood function of the state transition sequence  $\xi$ , i.e.,

$$\hat{\mathbf{X}} = \arg \max_{\xi} p(\mathbf{r}|\xi). \quad (16)$$

According to the trellis, each of the state transitions generates an output, also known as the noiseless read-back signal  $y_k$  and they have a one-to-one relationship. From (14), the received read-back signal  $r_k$  is equal to the signal of  $y_k$  plus the noise. If we assume that the noise components  $\{n_k\}$  are statistically independent, the read-back signal  $r_k$  are statistically independent random variable. Thereafter, the likelihood function of the state transition sequence  $\xi$ ,  $p(\mathbf{r}|\xi)$ , from (16) can also be expressed as

$$p(\mathbf{r}|\xi) = \prod_{k=1}^N p(r_k|\xi_k) = \prod_{k=1}^N p(r_k|y_k). \quad (17)$$

In here, the conditional probability density function  $p(r_k|y_k)$  can be computed as

$$p(r_k|y_k) = \frac{1}{\sqrt{2\pi\sigma^2}} \exp\left(-\frac{(r_k - y_k)^2}{2\sigma^2}\right), \quad (18)$$

where  $\sigma^2$  is the variance of the noise. For simplicity, the detector uses the log-likelihood function (logarithm of the likelihood function) and we have

$$\ln p(\mathbf{r}|\boldsymbol{\xi}) = -\frac{N}{2} \ln(2\pi\sigma) - \frac{1}{2\sigma^2} \sum_{k=1}^N (r_k - y_k)^2. \quad (19)$$

According to (19), the maximum of  $\ln p(\mathbf{r}|\boldsymbol{\xi})$  in MLSD is equivalent to the minimizing the Euclidean distance  $\sum_{k=1}^N (r_k - y_k)^2$ , also known as the path metric in the Viterbi algorithm. The Viterbi detector estimates the input symbol sequence based on the minimum *Euclidean distance* or the path metric through the trellis sequence, i.e.,

$$M = \sum_{k=1}^N (r_k - y_k) \quad (20)$$

After recovering the whole sequence of the input symbols, the detector extracts the estimated recorded bit sequence from the output symbol sequence. In this detection scheme, the complexity in the 2-D Viterbi detector will increase exponentially with the number of ITI and ISI taps in the channel. Therefore, this 2-D Viterbi detector is infeasible to implement in hardware due to excessive complexity.

## Chapter 3

### Joint Signal Processing Scheme for Multi-head Multi-track Read Channel

#### 3.1 Multi-track Joint Viterbi Detector for Multi-head Multi-track Read Channel

Normally, the Multi-head multi-track read channel system aims to mitigate the ITI effects on the readback signals by processing the signals from the side tracks so as to estimate the recorded data on the detecting tracks effectively. Most of earlier proposed MHMT systems usually do not attempt to recover the data from the side tracks because it is assumed that the readback signals do not contain enough contributions of side tracks to be recovered. In contrast, the researchers in [26] proposed an iterative multi-track detection concatenated with multiple decoders to recover the data from the side tracks also by processing just the signals from the detecting tracks and proved that the proposed system can estimate the data on the side tracks with a reasonable reliability. While the areal density of BPMR is increased further in the future, the intensity of ITI effect on the readback signal will be higher. Therefore, instead of attempting to mitigate the ITI, employing a robust 2-D data recovery system such as the multi-track joint 2-D detector can estimate the data on the side tracks from the readback signals while estimating the data on the detecting track so that the throughput capacity of MHMT can be increased and the estimated data from the side tracks can be used in further process.

In this work, we aim to study the performance of a multi-track joint 2-D Viterbi detector in conjunction with the multi-track 2-D equalization for estimating the recorded data on the side tracks for the high areal density of BPMR system. In the system, the equalized signals from the detecting tracks are processed by the detector for estimating the data on the detecting tracks and the side tracks concurrently. Since the indistinguishable symbols, due to the symmetric ITI effects, can degrade the performance of the detector, we propose to set the head offsets into the direction of the side track in the design of multi-head array. Moreover, it can increase the contribution from the side track on the readback signals. Then, we investigate the performance changes by that adjusting the head offset positions. The simulation results show that the data recovery performance of the side tracks can be improved without significant losing the performance of the detecting tracks at the optimal head offset positions.

### 3.1.1 Four-head four-track Equalization and Detection

In this work, we consider a four-head four-track (4H4T) read channel of the BPMP system with an array of four heads as shown in Fig.8. In the system, an array with four heads detects the bit islands on four adjacent tracks,  $l \in \{1, 2, 3, 4\}$  concurrently as depicted in Fig.8, and then generates four readback signals, i.e.,  $r_{1,k}$ ,  $r_{2,k}$ ,  $r_{3,k}$  and  $r_{4,k}$ .

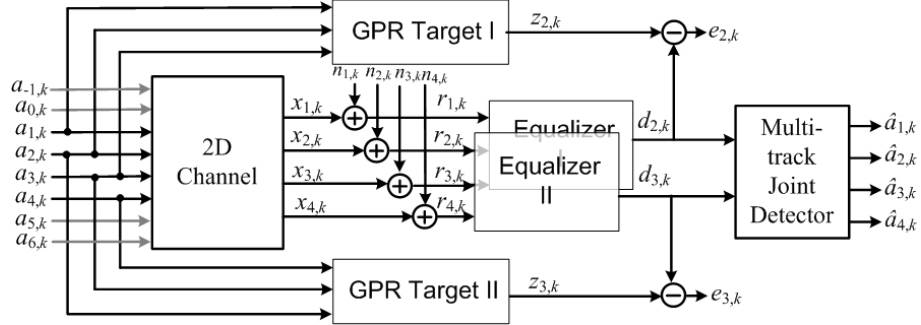


Fig. 8. The model of 4H4T BPMP channel with multi-track 2-D equalization and a multi-track joint 2-D detector.

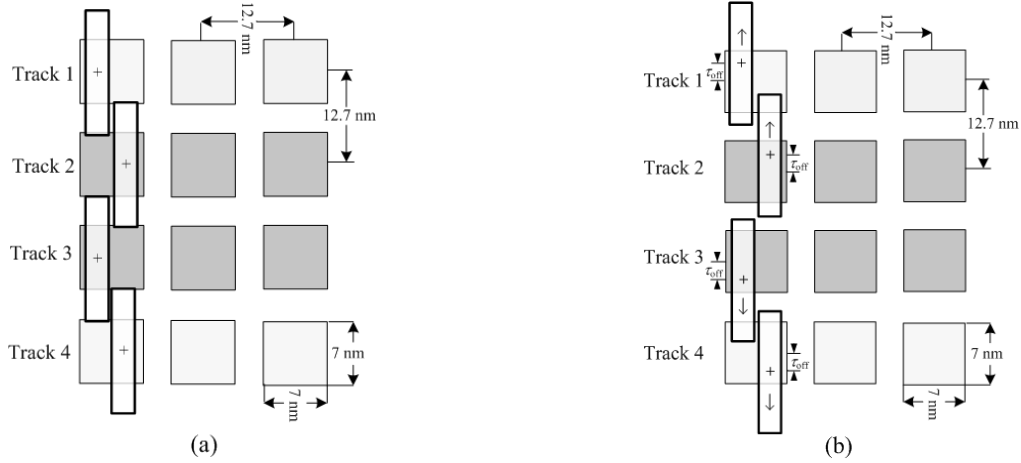


Fig. 9. The configuration of four heads (a) without head offset. (b) with head offset according to the direction of arrows.

The configurations of the head array with and without the head offset are shown in Fig. 9. In Fig. 9(a) the center of each head is aligned with that of the tracks when the value of  $\tau_{off}$  is zero. In this work, we propose to shift the heads on the tracks 1 and 2 into upward direction and the heads on the tracks 3 and 4 are in downward direction by the value of  $\tau_{off}$  as illustrated

the arrows in Fig. 9(b). It results higher ITI from the side tracks, but less from other detecting track onto the signals  $r_{2,k}$  and  $r_{3,k}$ . The negative value of  $\tau_{off}$  means the reverse offset movement of heads so that the readback signals will have more ITI from other detecting track but less from the side tracks.

In the system, the readback signals are sent to respective 2-D equalizers as depicted in Fig. 8. The Equalizer I generates the equalized signal  $d_{2,k}$  by processing the signals,  $r_{1,k}$ ,  $r_{2,k}$  and  $r_{3,k}$ , and the Equalizer II generates  $d_{3,k}$  by processing the signals,  $r_{2,k}$ ,  $r_{3,k}$  and  $r_{4,k}$ . Thereafter, two equalized signals are fed to a multi-track joint 2-D detector to generate the estimated recorded data sequences,  $\{\hat{a}_{1,k}\}$ ,  $\{\hat{a}_{2,k}\}$ ,  $\{\hat{a}_{3,k}\}$  and  $\{\hat{a}_{4,k}\}$ . In here, notice that even though all readback signals are fed into the two equalizers, only the equalized readback signals,  $d_{2,k}$  and  $d_{3,k}$  are processed by the detector and the signals,  $r_{1,k}$  and  $r_{4,k}$  are just utilized to equalize the  $r_{2,k}$  and  $r_{3,k}$  according to the 2-D generalized partial response (GPR) targets. Thus, the tracks, 2 and 3 are described as the detecting tracks and the tracks, 1 and 4 as the side tracks hereafter. For the detector, a full-fledged trellis is designed embedding the data bits on all four tracks (including the detecting tracks and the side tracks) to be estimated. Since the detector processes only two equalized signals the error rate in the sequences,  $\{\hat{a}_{1,k}\}$  and  $\{\hat{a}_{4,k}\}$  are expected to be higher than that of the sequences  $\{\hat{a}_{2,k}\}$  and  $\{\hat{a}_{3,k}\}$ . However, we investigate the performance changes of each estimated sequences by adjusting different head offset positions and search the optimal positions.

### 3.1.2 Multi-track 2-D Equalizer and 2-D GPR Target Approach

In order to control the ITI effects on each readback signal, we consider two 2-D equalizers with the size of  $3 \times (2L + 1)$  together with two 2-D GPR targets with the size of  $3 \times 3$ . The equalizer matrix  $\mathbf{F}_I$  and the GPR target matrix  $\mathbf{G}_I$  are defined as

$$\mathbf{F}_I = \begin{bmatrix} f_{-1,-N} & \cdots & \cdots & \cdots & \cdots \\ f_{0,-N} & \cdots & \cdots & \cdots & \cdots \\ f_{1,-N} & \cdots & \cdots & \cdots & \cdots \end{bmatrix} \quad (21)$$

and

$$\mathbf{G}_I = \begin{bmatrix} g_{-1,-1} & g_{-1,0} & g_{-1,1} \\ g_{0,-1} & g_{0,0} & g_{0,1} \\ g_{1,-1} & g_{1,0} & g_{1,1} \end{bmatrix}, \quad (22)$$

where  $l \in \{I, II\}$  is the index of the equalizer and the target. Each pair of 2-D equalizer  $\mathbf{F}_l$  and 2-D target  $\mathbf{G}_l$  are designed based on MMSE technique using the respective error sequence  $e_{l,k}$   $l \in \{2, 3\}$  is expressed by,

$$\begin{aligned} E\{e_{l,k}^2\} &= E\left\{\left(z_{l,k} - d_{l,k}\right)^2\right\} \quad \text{where } l \in \{2, 3\} \\ &= E\left\{\left(\sum_{m=-1}^1 \sum_{n=-L}^L f_{m,n} r_{l+m,k-n} - \sum_{m=-1}^1 \sum_{n=-1}^1 g_{m,n} a_{l+m,k-n}\right)^2\right\} \end{aligned} \quad (23)$$

where  $E\{\cdot\}$  is the expectation and  $e_{l,k}$  is the error signal.

### 3.1.3 Multi-track Joint 2-D Detector

In this work, a multi-track joint 2-D detector uses a full-fledged 2-D trellis constructed by considering the input bits from all four consecutive tracks (two detecting tracks and two side tracks) to be estimated. Therefore, in the trellis, each input symbol is defined as  $\mathbf{a}_k = \{a_{1,k}, a_{2,k}, a_{3,k}, a_{4,k}\}$  and then each state is composed by two symbols based on the given 2-D GPR targets. As a result, the 2-D trellis contains  $2^{4 \times 2} = 256$  states and  $2^4 = 16$  incoming or outgoing branches at each state. Considering the log-likelihood method, the computation of branch metric for each transition of the trellis can be simplified as

$$\mu_{\xi} = - \quad - \quad - \quad - \quad (24)$$

where  $d_{l,k}$  and  $z(\xi_k)$  are the equalized signal and target output of  $l \in \{2, 3\}$  tracks, and  $\xi_k$  represents the state transition between the current state  $S_k$  at time  $k$  and the next state  $S_{k+1}$  at time  $k+1$ . For branch metric in (7), each of target outputs is computed with the coefficients of the respective GPR target I and II. Using the Viterbi algorithm, the detector finally generates the estimated recorded bit sequences  $\{\hat{a}_{1,k}\}$ ,  $\{\hat{a}_{2,k}\}$ ,  $\{\hat{a}_{3,k}\}$  and  $\{\hat{a}_{4,k}\}$  by processing using the two equalized signals  $d_{2,k}$  and  $d_{3,k}$  that contain the significant ITI contributions from tracks 1 and 4.

### 3.1.4 Numerical Evaluation

Firstly, we observe the changes of the main ITI coefficients in the channel matrix by the head on the track 2 for the different head offset position which is defined as the ratio of head offset position to the track pitch, i.e.,  $\tau_{off}/T_z$  in Table I. The value of the upper ITI coefficients will rise and the value of the lower ITI coefficients will fall when the value of ratio is changed from the negative values to the positive values. The changes of the ITI coefficients in the matrices generated by the heads on the tracks 1 will be in the same manner but those on the tracks 3 and 4 will generate inversely as they are offset in opposite direction.

Table.1. The ITI Contributions Vs. Head Offset

Head Offset ( $\tau_{off}/T_z$ )	ITI coefficients [ $h_{2,0}$ , $h_{1,0}$ , $h_{0,0}$ , $h_{1,0}$ , $h_{2,0}$ ]
-0.15	[0.015, 0.305, 1, 0.527, 0.045]
-0.10	[0.018, 0.334, 1, 0.481, 0.037]
-0.05	[0.021, 0.365, 1, 0.439, 0.031]
0	[0.026, 0.401, 1, 0.401, 0.026]
0.05	[0.031, 0.439, 1, 0.365, 0.021]
0.10	[0.037, 0.481, 1, 0.334, 0.018]
0.15	[0.045, 0.527, 1, 0.305, 0.015]

Then we investigate the data estimating performances of the 4H4T system using a multi-track joint 2-D detector from the detecting tracks, i.e., the track 2 and 3, and from the side tracks, i.e., the track 1 and 4 at the SNR level of 18 dB for various head offset values and the simulation results are shown in Fig. 10. According to the results, the detector can improve the performance of estimating the data on the side tracks without significantly affecting on the estimating data on the detecting tracks when the upper two heads are offset away from the lower two heads because the detecting signals,  $r_{2,k}$  and  $r_{3,k}$  contain the more contributions from the side tracks 1 and 4. After the ratio value of 0.08, their performance starts to decline again because of the significant performance degrading of the detecting tracks. Therefore, we assume the optimal performance of data estimating from all four tracks is achieved when each pair of heads are shifted away from another pair by about  $0.08 T_z$ .



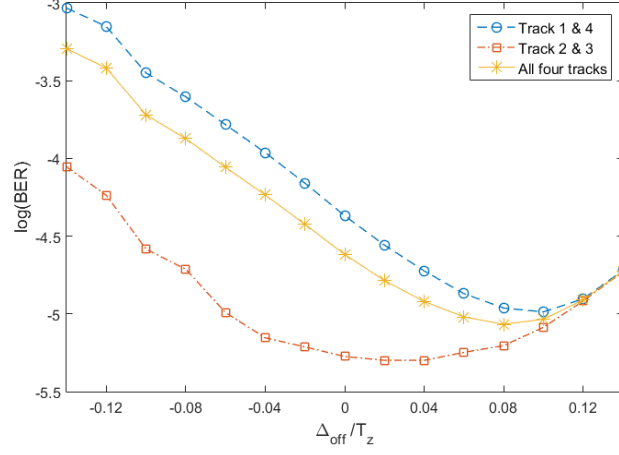


Fig. 10. Performance of estimating the data on the detecting tracks 2 & 3 and the side tracks 1 & 4 based on different head offset values at SNR 18dB.

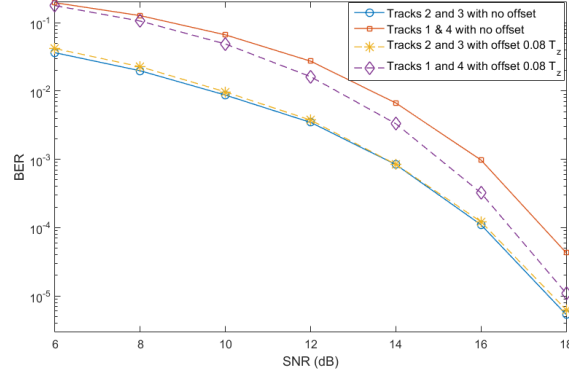


Fig. 11. The performance of estimating the data on the detecting tracks and the side tracks with and without the optimal head offset positions.

Finally, the bit error rate (BER) performance of the 4H4T system with no head offset and with the head offset position at  $0.08 T_z$  are compared in Fig. 11. In Figure, the performance of the data estimation from the detecting tracks and the side tracks are plotted separately. For the detecting tracks, the performance of the system with the head offset is insignificantly degraded compared to that of the system without the head offset because of the higher ITI effects. However, in contrast, the performance of the data estimating form the side tracks by the system with head offset is better than the system with no head offset. The former can provide the performance gain about 0.8dB at BER  $10^{-4}$ . This performance gain is achieved by the higher contributions from the side tracks as well as the asymmetric GPR targets which are designed using the MMSE methods for the asymmetric channel matrix.

### 3.2 Reduced Complexity Multi-track Joint Viterbi Detector for MHMT Channel

In this paper, we propose a multi-track joint Viterbi detector using a reduced complexity trellis to recover the recorded data bits from the detecting tracks as well as the sidetracks for the high areal density BPMR with multi-head multi-track (MHMT) systems, particularly a four-head four track (4H4T) system. In the system, the 2-D equalizers equalize the readback signals to 2-D generalized partial response (GPR) targets in which some ITI coefficients are set to zero in order to reduce the number of states in the trellis. The equalizers and targets are concurrently designed by minimizing the mean squared error (MSE). The parallel branches are incorporated into the trellis to estimate the data on sidetracks. With anticipation that each readback signal contains the substantial contributions from the sidetracks, the proposed system can generate the estimated data from the sidetracks with the acceptable reliabilities. Moreover, we propose a two-head four-track (2H4T) system using the proposed detector. Although it receives the signals from two detecting tracks only, the data on sidetracks can be estimated.

#### 3.2.1 Two MHMT channels (4H4T and 2H4T)

To estimate the recorded bits from the detecting tracks, most MHMT systems need the readback signals from both the detecting tracks and the sidetracks because the equalization system utilizes the sidetrack's signals to control the ITI effects on the readback signals. Therefore, the number of the estimating tracks by the MHMT systems is usually fewer than the number of tracks needed by the equalization. In contrast, we consider two MHMT systems: 4H4T system and 2H4T system, in this work. In both systems, we employ a multi-track joint equalization method to equalize the readback signals to the GPR targets with the ITI constraints.

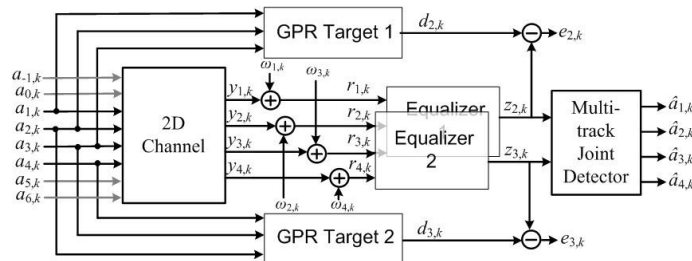


Fig. 12. The models of BPMRs 4H4T channel with the multi-track joint equalization and the proposed multi-track joint detector

The 4H4T system that receives the signals from the four tracks and generates the estimates of those four tracks is shown in Fig. 12. In this system, four readers sense the readback signals,  $r_{i,k}$ , from four consecutive tracks: the two detecting tracks, i.e., the track 2 and the track 3, and the two sidetracks, i.e., the track 1 and the track 4. Assuming that each readback signal is affected by the ITI effects from the two adjacent tracks above and two tracks below the middle track, the signal,  $r_{2,k}$ , has the contributions mainly from the bit on the track 2,  $a_{2,k}$ , as well as partially from the bits on the tracks 1 and 3,  $a_{1,k}$  and  $a_{3,k}$  (insignificantly from the tracks 0 and 4). Similarly, the readback signal,  $r_{3,k}$ , contains the contributions from the bits on the tracks 2, 3 and 4, i.e.,  $a_{2,k}$ ,  $a_{3,k}$  and  $a_{4,k}$ . In here, it is important to note that the signals from the sidetracks are used only in the equalizers, not in the detector. The 2-D equalizer  $\mathbf{F}_1$  equalizes the signal  $r_{2,k}$  according to the 2-D GPR target  $\mathbf{G}_1$  using the signals  $r_{1,k}$  and  $r_{3,k}$  as its sidetracks and then generates the equalized signal  $d_{2,k}$ . Similarly, the 2-D equalizer  $\mathbf{F}_2$  generates the equalized signal  $d_{3,k}$  by processing the signals,  $r_{2,k}$ ,  $r_{3,k}$  and  $r_{4,k}$ . Thereafter, the multi-track joint detector recovers the recorded data bits from all four tracks, from 1 to 4, by processing these two equalized signals.

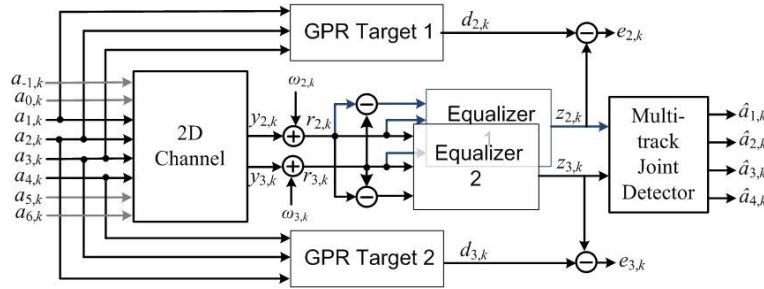


Fig. 13. The models of BPMRs 2H4T channel with the multi-track joint equalization and the proposed multi-track joint detector

As a simplified MHMT system, we also devise a 2H4T system that receives the signals from two tracks and estimates the recorded bits on four tracks as illustrated in Fig. 13. In the system, the equalizers receive the readback signals  $r_{2,k}$  and  $r_{3,k}$  from the two readers but no signals from the sidetracks. Since the equalizers equalize the readback signals  $r_{2,k}$  and  $r_{3,k}$  according to the respective 2-D GPR target that intends to include the ITI coefficients of the sidetracks, i.e., the track 1 or the track 4 as to be discussed in the next section, the equalizers still need the third input signal that include the information of the recorded bits on the sidetrack 1 or 4. Therefore, we generate a new signal sequence which is the difference between

two readback signals, i.e.,  $r_{2,k}$  and  $r_{3,k}$  and it is fed to both equalizers to help the equalizing process in this 2H4T system. Then, the multi-track joint detector estimates the recorded bits from all four tracks.

### 3.2.2 Multi-track Joint Equalizer and 2-D GPR target Design for Reduced Complexity Trellis

In both above systems, we employ two multi-track joint equalizers (21) to equalize the respective readback signals according to the 2-D GPR targets (22). For the proposed detector, we impose the constraints on the targets. Particularly, the coefficients of  $g_{-1,-1}$  and  $g_{-1,1}$  in  $\mathbf{G}_1$  and  $g_{1,-1}$  and  $g_{1,1}$  in  $\mathbf{G}_2$  are set to zero (to reduce the complexity of trellis) and the coefficient  $g_{0,0}$  in both targets to 1. By minimizing the MSE in (23), each pair of the equalizer and the target can be obtained from

$$\bar{\mathbf{g}}_I = (\mathbf{R}_a - \mathbf{R}_{ra}^T \mathbf{R}_r \mathbf{R}_{ra})^{-1} \mathbf{E}_I \boldsymbol{\lambda}_I, \quad (24)$$

$$\bar{\mathbf{f}}_I = \mathbf{R}_r^{-1} \mathbf{R}_{ra} \bar{\mathbf{g}}_I, \quad (25)$$

where  $\bar{\mathbf{g}}_I = [\mathbf{g}_{-1}, \mathbf{g}_0, \mathbf{g}_1]^T$  and  $\bar{\mathbf{f}}_I = [\mathbf{f}_{-1}, \mathbf{f}_0, \mathbf{f}_1]^T$  are the column vectors by rearranging the matrices in (3) and (4),  $\mathbf{R}_r$  is an auto-correlation matrix of the readback signal sequences from the three tracks involved,  $\mathbf{R}_a$  is an auto-correlation matrix of the recorded bit sequences on the three tracks involved, and  $\mathbf{R}_{ra}$  is the cross-correlation matrix of the readback signal sequences and the recorded bit sequences. In (6),  $\boldsymbol{\lambda}_I$  is a vector containing the Lagrange multipliers, i.e.,

$$\boldsymbol{\lambda}_I = \left( \mathbf{E}_I^T (\mathbf{R}_a - \mathbf{R}_{ra}^T \mathbf{R}_r \mathbf{R}_{ra})^{-1} \mathbf{E}_I \right)^{-1} \mathbf{c}_I, \quad (26)$$

where  $\mathbf{E}_I$  and  $\mathbf{c}_I$  are the vectors to impose the above constraints of  $\mathbf{G}_I$  so that  $\mathbf{E}_I \bar{\mathbf{g}}_I = \mathbf{c}_I$ . We set

$$\mathbf{E}_1 \text{ and } \mathbf{E}_2 \text{ to } \begin{bmatrix} 1 & 0 & 0 & 0 & 0 & 0 & \dots & - & - & \dots & 0 & 0 & 0 \\ 0 & 0 & 1 & 0 & 0 & 0 & \dots & | & | & \dots & 1 & 0 & 0 \\ 0 & 0 & 0 & 0 & 1 & 0 & \dots & - & - & \dots & 0 & 0 & 1 \end{bmatrix}^T$$

and  $\mathbf{c}_1$  and  $\mathbf{c}_2$  to  $[0 \ 0 \ 1]^T$  and  $[1 \ 0 \ 0]^T$ .

### 3.2.3 Multi-track Joint Detector with Reduced Complexity Trellis

In this work, we develop a multi-track joint 2-D detector with a reduced complexity trellis to recover the recorded bits from all of four tracks, i.e., from the tracks 1, an 4. Firstly, a

input symbol for the trellis is defined with the bits from the detecting tracks, i.e.,  $a_{2,k}$  and  $a_{3,k}$ . Based on the dimension of GPR targets, a state of the trellis is defined by two input symbols. As a result, the proposed trellis consists of  $2^{2 \times 2} = 16$  states and 4 possible next states from each state. The recorded bits from the side tracks, i.e.,  $a_{1,k-1}$  and  $a_{4,k-1}$ , are integrated into the trellis as the parallel branches in the state transition. With all the possible combinations of  $(a_{1,k-1}, a_{4,k-1}) \in \{(-1,-1), (-1,1), (1,-1), (1,1)\}$ , there are four parallel branches at each state transition, resulting to 16 outgoing branches from each state. The state transition diagram is shown in Fig. 14.

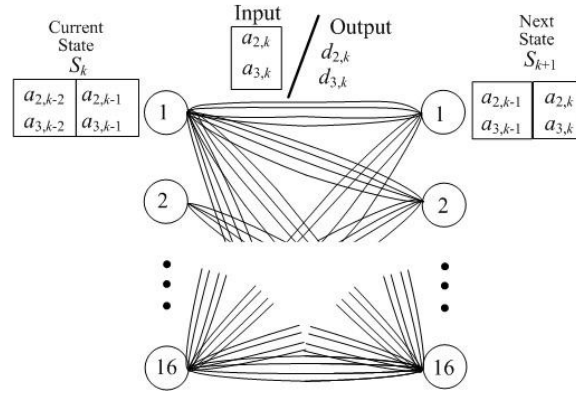


Fig. 14. The reduced complexity trellis for the multi-track joint detector.

Given that only AWGN noise is in the channel, the computation of the branch metric using the log-likelihood method for each parallel branch at each state transition of the trellis can be simplified as

$$\mu_{\xi} = - \sum_{l=2,3} \sum_{n=-1}^1 g_{m,n} z_{l,k} d(\xi_k) \quad (27)$$

where  $z_{l,k}$  and  $d(\xi_k)$  are the equalized signal and the desired signal with  $l \in \{2, 3\}$ , and  $\xi_k$  represents the state transition between the current state  $S_k$  at time  $k$  and the next state  $S_{k+1}$  at time  $k+1$ . With the coefficients of two GPR targets and the values of  $a_{1,k-1}$  and  $a_{4,k-1}$  of the given parallel branches, the desired signals are calculated as

$$d_2(\xi_k) = \sum_{m=0}^1 \sum_{n=-1}^1 g_{m,n} a_{2+m,k-n} + g_{-1,0} a_{1,k-1}, \quad (28)$$

and

$$d_3(\xi_k) = \sum_{m=-1}^0 \sum_{n=-1}^1 g_{n,m} a_{3+m,k-n} + g_{1,0} a_{4,k-1}. \quad (29)$$

While the Viterbi algorithm is finding the survivor path for each state at every state transition  $\xi_k$ , it computes the path metric for all parallel branches, and then selects the state transition which includes the parallel branch with the minimum path metric as a survivor. Thus, for each state at every state transition, the system needs to store the survivor state transition, its selected parallel branch and its path metric. After achieving the path with the minimum metric along the received signal sequence,  $\hat{a}_{2,k}$  and  $\hat{a}_{3,k}$  from the detecting tracks are generated based on the survivor state transition along the path, and  $\hat{a}_{1,k}$  and  $\hat{a}_{4,k}$  from the sidetracks are generated based on the selected parallel branch.

### 3.2.4 Numerical Results

For performance comparison, we consider a multi-track joint detector with the full-fledged trellis for the 4H4T system which has 256 states and 16 branches at each state. In the numerical simulations, we compute the bit error rates (BERs) of the detecting tracks based on the sequences  $\hat{a}_{2,k}$  and  $\hat{a}_{3,k}$  together and similarly the BERs of the sidetracks based on the sequences  $\hat{a}_{1,k}$  and  $\hat{a}_{4,k}$ . The performance comparison of the proposed detector in the 4H4T system and the 2H4T system to the full-fledged detector of the 4H4T system is shown in Fig. 15. For the estimated data from the sidetracks, the performance of the proposed detector is very close to that of the full-fledged detector in the 4H4T system; however, both detectors of the 4H4T systems are slightly inferior to the proposed detector of 2H4T system until about SNR = 18.3 dB and thereafter, significantly outperform to the 2H4T system. For the estimated data from the detecting tracks, the performance of the proposed detectors in the 2H4T system is progressively worse than that of both detectors in the 4H4T system because the 2H4T system receives only two readback signals. It is easy to notice that this shortfall in the 2H4T system affects the data estimated from the sidetracks.

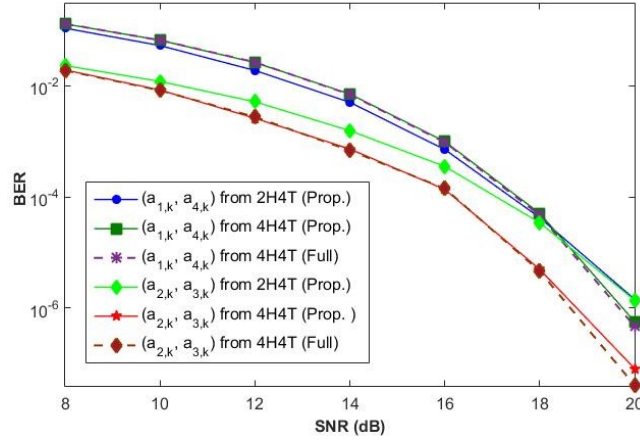


Fig. 15. Performance comparison of 4H4T system and 2H4T system using the proposed detector and the full-fledged detector for the BPMP system at the areal density 4 Tb/in<sup>2</sup>.

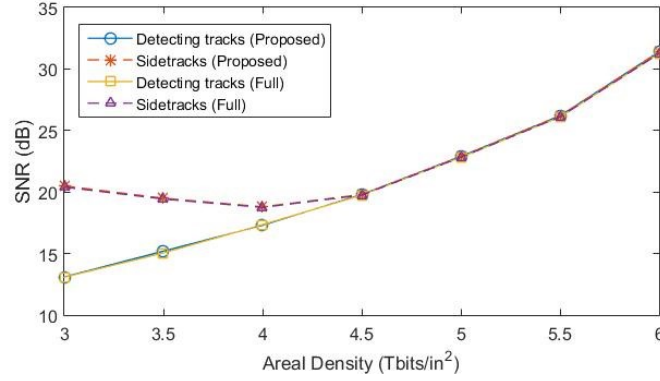


Fig. 16. The SNR required by the proposed and full-fledged detectors in the 4H4T systems to achieve BER = 10<sup>-5</sup> for the range of areal density.

The SNRs (dB) required by the proposed and full-fledged detectors in the 4H4T systems to achieve BER = 10<sup>-5</sup> at the areal densities from 3 Tb/in<sup>2</sup> to 6 Tb/in<sup>2</sup> are studied in Fig. 16. The proposed detector can perform as well as the full-fledged detector. From 4.5 Tb/in<sup>2</sup>, the performance of detecting tracks and sidetracks are very comparable due to the high ITI levels in the channel.

### 3.3 Noise Predictive Multi-track Joint Viterbi Detector

In MHMT channel, the output signals from 2-D equalizers are corrupted by the correlated/colored noise, and the performance of multi-track joint detector is not optimal due to it. In the literature, noise predictive detector is proposed to compensate the performance deficiency due to the colored noise [27-29]. Noise predictions for multi-track read channels are also studied in [30-31]. In a noise predictive detector, a linear noise predictor using finite impulse response (FIR) filter is employed to predict the current noise sample in terms of the most recent noise samples, and then, the predicted noise sample is used to correct the noise information in the branch metric calculation. Normally, the performance of linear noise predictor can be enhanced by increasing the number taps in filter, but it needs to extend the trellis structure or the feedback memory in the detector. However, integrating the noise prediction process into the multi-track joint detector can increase the computational complexity or more vulnerable to have propagation error. Alternatively, the noise predictor using infinite impulse response (IIR) filter is studied in [27]. In this work, we develop a noise predictive multi-track joint detector using FIR predictor and IIR predictor for multi-track BPMR read channel. Then, we study the performance of multi-track joint detector using predictors comparing with that of multi-track detectors without predictor for various areal densities of BPMR system.

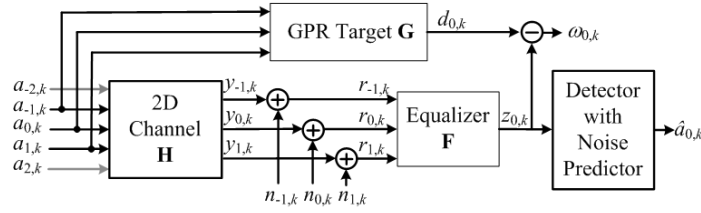


Fig. 17. The readback channel model of BPMR system.

#### 3.3.1 Noise Predictive Viterbi Detector

In the read channel as shown in Fig. 17, the equalized signal sample  $z_{l,k}$  for  $l = 0$  is

$$z_{l,k} = \sum_{i=-1}^1 \sum_{j=-L}^L f_{i,j} y_{l-i,k-j} + \sum_{i=-1}^1 \sum_{j=-L}^L f_{i,j} n_{l-i,k-j} \quad (30)$$

where  $y_{l,k}$  is the noiseless channel output signal sample and  $f_{i,j}$  is the coefficient of 2-D equalizer **F**. According to the second term in (30), the equalizer correlates the additive noise of



the received signals, and then the resulted noise becomes the colored noise which degrades the performance of Viterbi detector. However, this performance inferiority can be alleviated by integrating a noise predictor into the detector. In the noise predictor, the noise sample  $\omega_{l,k}$  is defined as the difference or error sample between the equalized readback signal sample,  $z_{l,k}$  and the desired output sample,  $d_{l,k}$ , i.e.,

$$\omega_{l,k} = z_{l,k} - d_{l,k}, \quad (31)$$

where  $d_{l,k}$  is computed with the coefficients  $g_{n,m}$  of the GPR target  $\mathbf{G}$ . It is important to notice that the noise sample  $\omega_{l,k}$  in (31) includes not only a correlated noise but also the residual interference due to mis-equalization. Since the noise sample is correlated with the neighboring samples due to the equalizer, the current noise sample can be predicted based on the past noise samples [27].

### 3.3.2 Noise Prediction Filter

In a linear predictor model, the predicted current noise sample can be defined as,

$$\hat{\omega}_{l,k} = \sum_{i=1}^K p_i \omega_{l,k-i}, \quad (31)$$

where  $\omega_{l,k}$  is a previous noise sample at time delay  $i$  from (30),  $p_i$  is the coefficient of the linear noise prediction FIR filter, and  $K$  is the length of the filter. To design the filter, the mean squared error (MSE) of the noise prediction error is defined as

$$E[\|\omega_{l,k} - \hat{\omega}_{l,k}\|^2] = E\left[\left\|\omega_{l,k} - \sum_{i=1}^K p_i \omega_{l,k-i}\right\|^2\right]. \quad (32)$$

The optimal coefficients of prediction filter  $p_i$  can be found by minimizing the mean squared error in (32) and as the solution of the normal equation [28]. Let  $\mathbf{p} = [p_1, p_2, \dots, p_K]^T$  be a column vector of the coefficients of the noise prediction filter and then it is expressed as,

$$\mathbf{p} = \mathbf{R}_{\omega\omega}^{-1} \mathbf{r}_{\omega\omega}, \quad (32)$$

Where  $\mathbf{r}_{\omega\omega} = E[\omega_{l,k} \omega]$  and  $\mathbf{R}_{\omega\omega} = E[\omega \omega^T]$  are an autocorrelation vector and an autocorrelation matrix of the noise samples sequence  $\omega = [\omega_{l,k-1}, \dots, \omega_{l,k-K}]^T$  respectively.

Alternatively, the noise sample can be predicted using an IIR filter. The IIR filter can provide the performance improvement without increasing the number of filter taps. Therefore, we also consider the IIR filter for noise prediction in this study. For IIR noise prediction, the predicted noise sample is written as a recursive equation, i.e.,

$$\hat{\omega}_{l,k} = \sum_{j=1}^K (\alpha_j + \beta_j) \omega_{l,k-j} - \sum_{j=1}^K \alpha_j \hat{\omega}_{l,k-j}, \quad (33)$$

where  $\alpha_j$  and  $\beta_j$  are the zero-pole parameters of the IIR filter, and  $K$  is the length of the filter. The zero-pole parameters in (33) can be calculated from the autocorrelation function of noise sample sequence as described in [27].

### 3.3.3 Noise Prediction based on stored value on Surviving Path

With the predicted noise sample, the branch metric of the Viterbi detector for a state transition at time  $k$  is modified as,

$$\lambda(S_{k-1}^m, S_k^n) = \left[ z_{l,k} - d(S_{k-1}^m, S_k^n) - \hat{\omega}_{l,k} \right]^2, \quad (34)$$

where  $S_{k-1}^m$  and  $S_k^n$  are the previous  $m^{th}$  state and the current  $n^{th}$  state at time  $k$  for  $m, n \in \{1, 2, \dots, M_s\}$ ,  $d_k(S_{k-1}^m, S_k^n)$  is the target output sample generated with the input bits of the branch and the bits defined in the state  $S_{k-1}^m$ , and  $M_s$  is the total number of states in the trellis. Based on (30) and (33), the predicted noise sample is computed with the previous noise samples, i.e.,  $\omega_{l,k-i}$  for  $i \in \{1, \dots, K\}$ , and the previous noise sample computation consequently requires a number of past input bits from three tracks, but they are beyond the input bits of the state  $S_{k-1}^m$  of the given trellis. Therefore, in the conventional technique, the trellis is redesigned based on the effective target  $G(D) = \mathcal{A}(D)[1 - \mathcal{P}(D)]$  to attain the previous noise samples, and the noise whitening filter,  $[1 - \mathcal{P}(D)]$  is added before the detector. However, this technique is not appropriate for the Viterbi detector of the 2-D interference channel because the complexity can lead into impractically high.

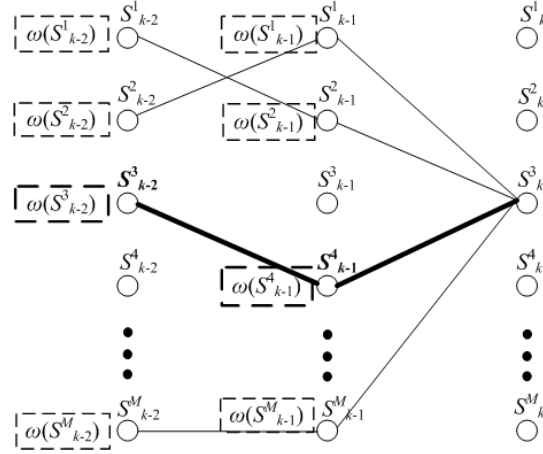


Fig. 18. The hypothetical surviving paths with stored noise samples for the proposed noise prediction technique.

In the proposed technique, the past noise samples are stored along the surviving paths for the noise prediction so that it doesn't need to extend the trellis. In particular, the Viterbi algorithm computes  $\omega_{l,k}$  which is the difference between the equalized signal sample  $z_{l,k}$  and the desired output sample  $d_k(S_{k-1}^m, S_k^n)$  of the state transition for the branch metric at time  $k$  in (34). In the proposed technique, this computed  $\omega_{l,k}$  is stored as the noise sample associated to that  $S_k^n$  state, i.e.,  $\omega(S_k^n)$  for the future noise prediction if its respective branch is selected as a part of the surviving path. Since the surviving path includes the sequence of most likely past states leading to the current state, those noise samples are most reliable information to predict the current noise. For the branch metric calculation at each transition, it is assumed that the prediction algorithm can access the stored information along the surviving path in depth of the length of the predictor. With the previous noise samples stored along the surviving path leading to the current state  $S_k^n$ , the branch metric equation in (34) is rewritten as,

$$\lambda(S_{k-1}^m, S_k^n) = \left[ z_{l,k} - d(S_{k-1}^m, S_k^n) - \sum_{i=1}^K p_i \omega(S_{k-i}^n) \right]^2, \quad (35)$$

For an example of a Viterbi detector the noise predictor of length  $K = 2$ , the system will read back two previous stages along the surviving path. The trellis with the hypothetical paths that stores the noise samples for this example is demonstrated in Fig. 18. When the branch metric of the transition from the previous state  $S_{k-1}^4$  to the current state  $S_k^3$  at time  $k$  is

computed, the predicted noise sample is estimated with the previous noise samples along the surviving path leading the current state through the previous state (the bold lines in Fig. 18), i.e.,  $\alpha(S_{k-1}^4)$  from the time  $k-1$ , and  $\alpha(S_{k-2}^3)$  from the time  $k-2$ . For other branch metric calculations, the current noise samples are predicted with the past noise samples along their respective surviving paths. Finally, the current noise sample  $\alpha(S_k^3) = z_{l,k} - d_k(S_{k-1}^4, S_k^3)$  is stored at the state  $S_k^3$  for further noise prediction if that branch is selected as a part of surviving path. Since the information along the surviving path are the most reliable, it is expected that the predicted noise samples based on them are also most reliable and enhance the performance of Viterbi detector.

The proposed noise prediction technique needs one extra storage for each state, and  $K$  more multiplications and additions for predicting the noise sample at each branch metric computation than the detector without noise predictor. As a result, the complexity increment of the proposed noise prediction technique is significantly less than the noise prediction by extending the trellis. However, this noise prediction technique needs a precaution for error propagation because the past noise samples are computed with the tentative estimates based on the most likelihood or on the surviving path.

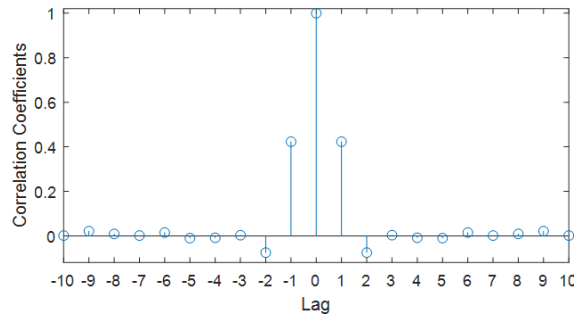


Fig. 19, the autocorrelation of the noise samples sequence  $\{w_{l,k}\}$ .

### 3.3.4 Simulation Result and Discussion

In this work, the 2-D channel response matrices with the size of  $5 \times 3$  at the areal densities of 3 Tbits/in<sup>2</sup> and 4 Tbits/in<sup>2</sup> are generated and employed for evaluating the proposed noise prediction. Firstly we study the autocorrelation function of the noise samples sequence  $\{w_{l,k}\}$  in (31) for the BPMP readback channel model. The autocorrelation function of the noise samples sequence of the BPMP channel at 4 Tbits/in<sup>2</sup> is shown in Fig. 19. It is obviously that the

noise samples sequence is correlated. Especially, the non-zero coefficients at first lags are the most significant and other coefficients are not as obvious as the coefficients of the first lags. Therefore, we employ the FIR noise predictor with only one tap and the IIR noise predictor with single-pole to avoid the error propagation problem. The coefficients of FIR noise prediction filter are computed with the autocorrelation functions of noise samples using (32) and the coefficients of IIR filter are computed like [27] using a known training sequence.

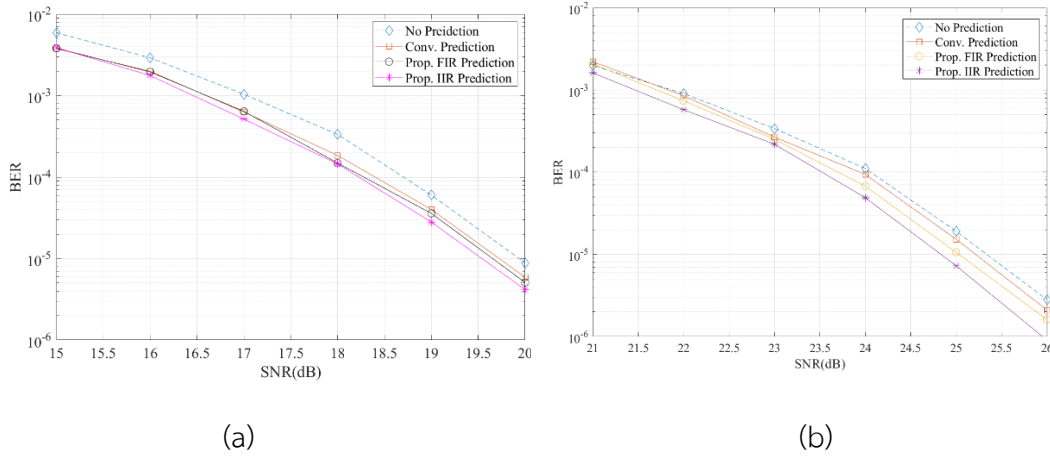


Fig. 20. Performance comparison of the Viterbi detectors with and without various noise prediction techniques for BPMR system with (a) 3 Tbit/in<sup>2</sup> and (b) 4 Tbit/in<sup>2</sup>

The bit error rate (BER) performances of the Viterbi detectors with the proposed prediction technique are compared to that of the detectors without noise predictor and with the conventional noise predictor that employs a extended trellis. The performance comparison of the detectors for the BPMR system of 3 Tbits/in<sup>2</sup> is shown in Fig. 20(a). All detectors with noise predictor provide better performance than the detector without noise predictor. The performance of the proposed noise prediction with FIR filter is not significant from that of conventional predictor, although the proposed noise prediction with IIR filter provides the best performance gain. At the areal density of 4 Tbits/in<sup>2</sup>, the detectors with the proposed noise prediction perform significantly better than others as depicted in Fig. 20(b). The detector with IIR predictor achieves the performance gain about 0.5 dB and the detector with FIR predictor about 0.4 dB over the detector with no noise predictor. In both areal densities, the noise prediction technique with extending trellis is inferior to the proposed techniques.

### 3.4 Track Mis-registration Estimation

By processing the multiple readback signals from the array of heads, TMR level can be predicted in the two-dimensional (2-D) joint equalization [31]. In [32], the head offset is computed based on the detector's output data sequences on the main track for the system with a single head and a 2x2 channel matrix by considering that the read head covers two tracks. The presence of TMR detection for a 3x3 channel matrix of BPMR system was proposed based on the observation of the 2-D target-shaping equalizer in [17], but it also still needs multiple readback signals from the adjacent tracks. However, this proposed method detects only the presence of TMR. In [24],[25], the TMR's level estimation method was proposed using the estimated SNR value and the average energy of the readback signal at the expense of intensive computing. We propose a simple TMR estimation method using the coefficients of a 2-D generalized partial response (GPR) target for a BPMR system. In the model, a 1-D equalizer and a 2-D GPR target are designed by a minimum mean squared error (MMSE) technique. Since the coefficients of both equalizer and target are computed optimally according to the channel, we can assume that the 2-D target, especially its side track coefficients, acquire the TMR information from the channel. Thereafter, the proposed method uses the coefficients of the resulted 2D GPR target to estimate the level of TMR. The relationship between the TMR and the coefficients is studied and then the TMR estimation equation is formulated with the help of a polynomial curve fitting technique.

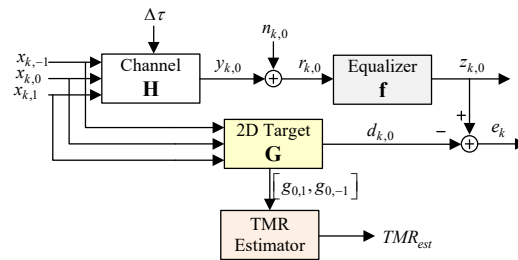


Fig.21. Block diagram of bit patterned media recording system.

The model of BPMR system with a TMR estimation method is shown in Figure 21. In the model, the three recording sequences, i.e.,  $\{x_{k,-1}\}$ ,  $\{x_{k,0}\}$  and  $\{x_{k,1}\}$  from the three adjacent tracks are sent to the 2-D BPMR channel. However, the sequence  $\{x_{k,0}\}$  from the main track is considered as the data sequence to be recovered and other two sequences from the adjacent

tracks are just for ITI effects in this work. The channel coefficients are generated by sampling a isolated island's pulse response at the integer multiples of the bit period and track pitch, i.e.,

$$h_{m,n} = P(-mT_x, -(nT_z + \Delta\tau)) \quad (36)$$

where  $P(x, y)$  is the 2-D Gaussian pulse response,  $T_x$  is the bit period,  $T_z$  is the track pitch and the  $\Delta\tau$  is the head offset or the distance between the center of the head and the center of the track as shown in Figure 22. In this paper, the TMR level is defined as

$$TMR(\%) = \frac{\Delta\tau}{T_z} \times 100. \quad (37)$$

When the system has no TMR impairment, the value of  $\Delta\tau$  is zero, giving a symmetric ITI effects (the same coefficients at the top and bottom rows) in the channel matrix from (37). With TMR, however, ITI will be asymmetric and the severity of ITI is depending on the value of  $\Delta\tau$ . The sign of  $\Delta\tau$  is positive for the upward offset, otherwise it is negative.

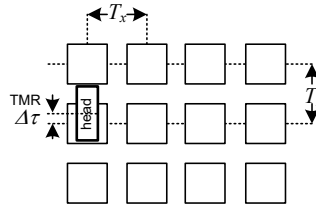


Fig. 22. The TMR effect in a BPMP system.

At the channel output, the readback signal sequence from the main track,  $\{r_{k,0}\}$ , from the channel is equalized with a 1-D equalizer  $\mathbf{f}$  to generate the equalized readback signal sequences  $\{z_{k,0}\}$  which is then processed by a detector integrated with TMR alleviation system will be considered in the further study. Firstly, the equalizer  $\mathbf{f}$  with the size of  $1 \times (2N + 1)$  and the 2-D PR target matrix  $\mathbf{G}$ , both are designed with MMSE technique, are defined as

$$\mathbf{f} = [f_{-N} \quad \cdots \quad \cdots \quad \cdots \quad \cdots] \quad (38)$$

$$\mathbf{G} = \begin{bmatrix} g_{-1,-1} & g_{0,-1} & g_{1,-1} \\ g_{-1,0} & g_{0,0} & g_{1,0} \\ g_{-1,1} & g_{0,1} & g_{1,1} \end{bmatrix}. \quad (39)$$

### 3.4.1 TMR Estimation Technique

When the BPMP system is experiencing with the TMR impairment, the asymmetric ITI effects are formed in the channel. It means the coefficients in the top and bottom rows of channel matrix  $\mathbf{H}$  become asymmetric. To detect the presence of TMR, [17] defined a ratio  $\phi$  by the value of those channel coefficients. While the value of ratio  $\phi$  varies according to the value of TMR level, the presence of TMR is detected by observing it. However, in practice, the values of the channel coefficients are unknown during the data recovery process; hence, the estimated values of the channel's coefficients are proposed to use with the high complexity of the computing.

We propose a simple TMR level estimating process using the coefficients of the GPR target matrix  $\mathbf{G}$  instead of the estimated channel coefficients. During the MMSE technique, the optimal 2-D GPR target and its 1-D equalizer are designed to match with the 2-D BPMP channel. Since the equalizer is a 1-D vector, the optimization technique computes the coefficients at the top row and bottom row of 2-D GPR target matrix until they are very close to those of the channel matrix. Therefore, when the channel poses with the TMR impairment, the value difference between the coefficients in those two rows in the target matrix are significantly obvious according to the severity of TMR. However, their values will be very close if there is no TMR. Based on this assumption, it is possible to retrieve the level of TMR or the head offset from the coefficients of the target  $\mathbf{G}$ .

In Here, a new ratio  $\beta$  is defined using the two center coefficients,  $g_{0,1}$  from the top row and,  $g_{0,-1}$  from bottom row of the target matrix (39), i.e.,

$$\beta = \frac{g_{0,1} - g_{0,-1}}{g_{0,1} + g_{0,-1}} \quad (40)$$

Similar to the ratio  $\phi$  in [17], the value of ratio  $\beta$  varies depending on the severity of the actual TMR level. Without TMR, it is very close to zero. When the TMR is happened, the TMR level and the offset direction can be estimated by observing its value. TMR is upward if  $\beta > 0$ , otherwise, it is downward.



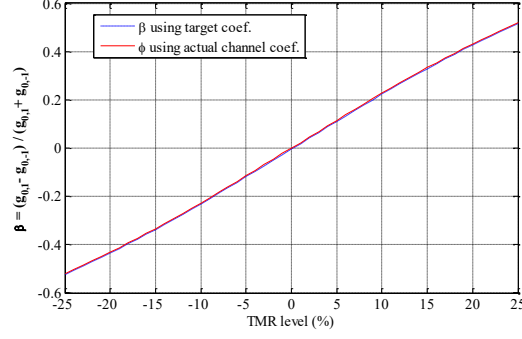


Fig.23. The values of ratio  $\beta$  at various level TMR in %.

To study the relationship between the value of ratio  $\beta$  and the value of TMR, the values of ratio  $\beta$  are firstly computed at various TMR levels including both upward and downward directions. In Fig. 3, the values of ratio  $\beta$  is plotted with the different TMR levels and compared with the values of ratio  $\phi$  which is computed by the coefficients of the actual channel matrix  $\mathbf{H}$ . According to Fig. 23, it is obviously noticed that the curves of  $\beta$  and  $\phi$  are almost identical over the various TMR levels and both of them are almost linear. Hence, it is proved that the TMR level can be estimated by observing the curve of  $\beta$ . Using on the data set of the computed values of  $\beta$  and their respective TMR level, a polynomial equation is modelled utilizing the polynomial curve fitting technique. According to empirical results, there is no accuracy improvement after 2<sup>nd</sup> order; therefore, a 2<sup>nd</sup> degree polynomial equation is used to estimate the TMR level, i.e.,

$$TMR_{est} = c_1\beta^2 + c_2\beta + c_3 \quad (41)$$

where  $c_1$ ,  $c_2$  and  $c_3$  are the coefficients of the 2<sup>nd</sup> degree polynomial equation generated by the polynomial curve fitting technique. Finally, the proposed method can estimate the TMR level with the value of  $\beta$  which is computed with the two coefficients of the target  $\mathbf{G}$ .

### 3.4.2 Simulation Result

The error percentage in the estimated TMR values from the proposed method is shown in Fig. 24. In here, the error percentage is calculated with the value of estimated TMR level and that of the actual TMR level, i.e.,

$$Error = \frac{|TMR_{est} - TMR_{actual}|}{TMR_{actual}} \times 100. \quad (42)$$

According to the results, the proposed method can estimate the TMR level accurately with small errors. From Figure 4, the error percentage is getting less while the TMR level is approaching to 20%, but the largest error percentage occurs at low TMR level range because the low TMR level has no significant effect on the channel. However, the proposed method can estimate the TMR level more accurately when TMR is getting more significant in the channel. In

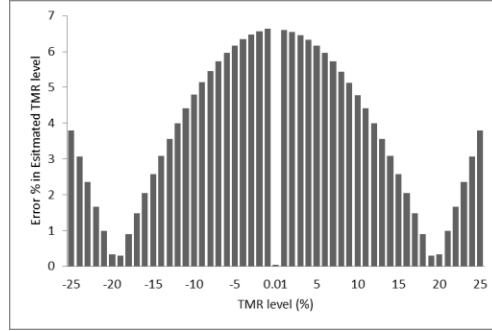


Fig. 24. The percentage of error of the estimated values from the proposed method.

## Chapter 4

### Conclusion

In this research project, we proposed a novel advanced joint signal processing scheme for the multi-head multi-track (MHMT) read channels to combat the system impairments such as the 2-D interference, the media noise and TMR in BPMR systems. Firstly, we investigated various configurations of MHMT recording systems and various trade-offs between performance and complexity for multi-track joint detection techniques including various reduced complexity methods for detector. For simplicity, readback channel models of the MHMT read channels with using two heads to detect two tracks and four tracks are developed for BPMR systems. We assume that the ITI contributions of the side tracks onto the readback signals are getting higher in the higher areal density of magnetic recording system, thus, it is expected that the robust detector with the help of multi-track signal processing can enable to estimate the recorded data from the side tracks by processing the signal from the detecting tracks. Therefore, we studied the performance of the recorded data estimation from the detecting tracks as well as the side tracks using a 4H4T BPMR system with multi-track 2-D equalization and a multi-track joint 2-D Viterbi detector. Employing a high complexity trellis, the system can estimate the data on the detecting tracks and the side tracks well by processing the readback signals from detecting tracks when the heads are offset optimally. There is a performance gap between the side tracks and the detecting tracks; however, it can be narrowed by further processing with the error control coding such as LDPC code in the system. Then, a multi-track joint detection technique with practicable low complexity level is devised with the help of equalization and MHMT recording technology.

In this project, we also developed noise predictive Viterbi detectors with low complexity for the 2-D interference channel of high areal density BPMR system. To avoid the high complexity, we proposed a noise prediction technique in which the current noise sample is estimated using the past noise samples sequence that stored along the surviving path. For noise prediction filter, we consider one filter tap for FIR filter and a single-pole for IIR filter to minimize the error propagation. The simulation results show that the detectors with proposed

noise prediction technique can provide the performance gain over the detectors without noise predictor and with the conventional noise predictor by extending the trellis. Finally, a TMR estimation technique is designed based on the coefficients of MMSE GPR targets and the performance of the proposed TMR estimation is compared with the conventional methods.

As a further study, we are developing on a patterned depend noise predictive detector using the proposed noise prediction technique. Moreover, we will integrate the propose TMR estimation technique into the low complexity multi-track joint detector to compensate the performance loss.

## Reference

- [1] R.Wood, "The feasibility of magnetic recording at 1 terabit per square inch," *IEEE Trans. Magn.*, vol. 36, pp. 36–42, Jan. 2000.
- [2] B. Terris, T. Thomson, and G. Hu, "Patterned media for future magnetic data storage," *Microsyst. Technol.*, vol. 13, no. 2, pp. 189–196, Nov. 2006.
- [3] W. Chang and J. R. Cruz, "Inter-track interference mitigation for bit patterned magnetic recording," *IEEE Trans. Magn.*, vol. 46, no. 11, pp. 3899–3908, Nov. 2010.
- [4] S. Karakulak, P. Siegel, J. K. Wolf, and H. N. Bertram, "Join-track equalization and detection for bit patterned media recording," *IEEE Trans. Magn.*, vol. 46, no. 9, pp. 3639–3647, Sep. 2010.
- [5] S. Koonkarnkhai, P. Keeratiwintakorn, and P. Kovintavewat, "Target and equalizer design for high-density bit-patterned media recording," *ECTI Trans. CIT.*, vol. 6, no. 2, Nov. 2012.
- [6] S. Nabavi and B. V. K. Vijaya Kumar, "Two-dimensional generalized partial response equalizer for bit-patterned media," in *Proc. IEEE Int. Conf. Commun. (ICC)*, 2007, pp. 6249–54.
- [7] L. Myint, P. Supnithi, and P. Tantaswadi, "An Inter-Track Interference Mitigation Technique Using Partial ITI Estimation in Patterned Media Storage," *IEEE Trans. Magn.*, vol. 45, no. 10, pp. 3691–3694, Oct. 2009.
- [8] J. Kim and J. Lee, "Iterative two-dimensional soft output Viterbi Algorithm for Patterned Media," *IEEE Trans. Magn.*, vol. 47, no. 3, pp. 594–597, March. 2011.
- [9] A. Hekstra, W. Coene and A. Immink, "Refinements of multi-track viterbi bit-detection," *IEEE Trans. Magn.*, vol. 43, no. 7, July 2007.
- [10] N. Zheng, K.S. Venkataranman, A. Kavcic and T. Zhang, "A study of multitrack joint 2-D signal detection performance and implementation cost for shingled magnetic recording," *IEEE Trans. Magn.*, vol. 50, no. 6, pp. 3100906, June 2014.

- [11] G. Mathew, E. Hwang, J. Park, G. Garfunkel and D. Hu, "Capacity advantage of array-reader-based magnetic recording (ARMR) for next generation hard disk drives," *IEEE Trans. Magn.*, vol. 50 no. 3, Mar., 2014.
- [12] B. Fan, H. Thapar and P. Seigel, "Multihead multitrack detection with reduced-state sequence estimation," *IEEE Trans. Magn.*, vol. 51, no. 11, pp. 3001404, Nov. 2015.
- [13] Y. Wang and B.V.K.V Kumar, "Multi-track joint detection for shingled magnetic recording on bit patterned media with 2D sectors," *IEEE Trans. Magn.*, vol. 52, no. 7, pp. 3001507, June. 2016.
- [14] S. Nabavi, B. V. K. Vijaya Kumar, J. A. Bain, C. Hogg, and S. A. Majetich, "Application of Image Processing to Characterize Patterning Noise in Self-Assembled Nano-Masks for Bit-Patterned Media," *IEEE Trans. Magn.*, vol. 45, pp. 3523-3526, Oct. 2009.
- [15] P.W. Nutter, I. T. Ntokas, and B.K. Middleton, "An Investigation of the Effects of Media Characteristics on Read Channel Performance for Patterned Media Storage," *IEEE Trans. Magn.*, vol. 41, pp. 4327-4334, Nov. 2005.
- [16] Y. Ng, K. Cai, B.V.K.V. Kumar, S. Zhang and T. C. Chong "Modeling and two-dimensional equalization for bit-patterned media channels with media noise," *IEEE Trans. Magn.*, vol. 45, no. 10, pp. 3535 – 3538, Oct. 2009.
- [17] L. Myint and P. Supnithi "Off-track detection based on the readback signals in magnetic recording," *IEEE Trans. Magn.*, vol. 48, no. 11, pp. 4590 – 4593, Oct. 2009.
- [18] J. Moon and W. Zeng, "Equalization for maximum likelihood detector," *IEEE Trans. Magn.*, vol. 31, no. 2, pp. 1083 – 1088, March 1995.
- [19] G. D. Forney, Jr., "Maximum-likelihood sequence estimation of digital sequences in the presence of intersymbol interference," *IEEE Trans. Inform. Theory*, vol. IT-18, no. 3, pp. 363-378, May 1972.

- [20] H. Burkhardt, "Optimal data retrieval for high density storage," in Proc. IEEE CompEuro '89 Conf. VLSI Computer Peripherals. VLSI and Microelectronic Applications in Intelligent Peripherals and Their Interconnection Networks, 1989, pp. 43-48.
- [21] B.Vucetic and, J. Yuan, Turbo Codes: Principles and Applications, 2nd de. Kluwer Academic Publisher , 2000.
- [22] S. Nabavi, V. Kumar, and J. G. Zhu, "Modifying Viterbi algorithm to mitigate intertrack interference in bit-patterned media," *IEEE Trans. Magn.*, vol. 43, no. 6, pp. 2274-2276, Jun. 2007.
- [23] L. Myint and C. Warisarn, "Equalizer design for bit-patterned media recording system Based on ISI and ITI estimations by cross correlation functions," *Journal of Applied Mechanics and Materials*, vol 781, pp 223-226, Aug., 2015.
- [24] W. Busyatras, A. Arrayangkool, C. Warisarn, L. M.M. Myint, P. Supnithi, and P. Kovintavewat, "An iterative TMR mitigation method based on readback signal for bit-patterned media recording," *IEEE Trans. Magn.*, vol.51 no. 11, Nov., 2015.
- [25] W. Busyatras, A. Arrayangkool, C. Warisarn, L. M.M. Myint, P. Supnithi, and P. Kovintavewat, "A TMR mitigation method based on readback signal in bit-patterned media recording," *IEICE Trans. Electron.*, vol. e98-C, no. 8, Aug. 2015.
- [26] G. Han, Y. L. Guan, K. Cai and K. S. Chan, "Asymmetric Iterative Multi-Track Detection for 2-D Non-Binary LDPC-Coded Magnetic Recording," *IEEE Trans. Magn.*, vol. 49, no. 10, pp. 5215-5221, Oct. 2013.
- [27] J. D. Coker, E. Eleftheriou, R. L. Galbraith, and W. Hirt, "Noise Predictive Maximum Likelihood (NPML) Detection," *IEEE Trans. Magn.*, vol. 34, no. 1, pp. 110-117, 1998.
- [28] J. Caroselli, S. A. Altekarak, P. McEwen and J. K. Wolf, "Improved Detection for Magnetic Recording Systems with Media Noise," *IEEE Trans. Magn.*, vol. 33, no. 5, pp. 2779-2781, Sept. 1997.

- [28] J. Moon and J. Park, "Pattern-dependent Noise Prediction in Signal Dependent Noise," *IEEE J. Select. Areas on Commn.*, vol. 19, no. 4, pp. 730-743, 2001.
- [29] Y. Wang and B. V. Kumar, "Multi-track Joint Detection for Shingled Magnetic Recording on Bit Patterned Media with 2-d Sectors," *IEEE Trans. Magn.*, vol. 52, no. 7, pp. 1-7, 2016.
- [30] S. Shi and J. R. Barry, "Multitrack Detection with 2D Pattern-Dependent Noise Prediction," *Proc. IEEE ICC*, Kansas City, MO, 2018, pp. 1-6.
- [31] S. Nabavi, B V.K.V. Kumar and J. Bain, "Mitigating the effects of track mis-registration in bit-patterned media," in *Proc. IEEE Int. Conf. Commun.* 2008, pp. 1061-2065, May 2008.
- [32] B.G. Roh, S.U. Lee, J. Moon and Y. Chen, "Single-head/single-track detection interfering tracks," *IEEE Trans. Magn.*, vol. 38, no. 4, pp. 1830-1838, July 2002.



## Appendix:

### Publication List

#### International Journal

1. L. M.M. Myint, C. Warisarn, P. Supnithi “Reduced Complexity Multi-track Joint Detector for Sidetrack Data Estimation in High Areal Density BPMR,” to be published in IEEE Transactions on Magnetics, vol. 54, no. 11, pp. 1-5, Nov 2018. (Impact factor = 1.386).

#### International Conferences

2. L. Myint, C. Warisarn, and P. Supnithi, “Reduced Complexity Multi-track Joint Equalization and Detection of High Areal Density Magnetic Recording,” Digest of IEEE International Magnetics Conference 2018 (INTERMAG 2018), Singapore. (April 25-27, 2018)
3. L. Myint, and P. Supnithi, “Sidetrack Data Estimation Using Multi-track Joint 2-D Viterbi Detector in Bit Patterned Media Storage,” 2018 15th International Conference on Electrical Engineering/Electronics, Computer, Telecommunications and Information Technology (ECTI-CON 2018), Chiang Rai, Thailand, July 2018.
4. L. Myint, and P. Supnithi, “Study of Detectors with Noise Predictor of High Areal Density BPMR Systems,” 2019 11th International Conference on Knowledge and Smart Technology (KST 0219), Phuket, Thailand, Jan. 2019.

# Reduced Complexity Multi-Track Joint Detector for Sidetrack Data Estimation in High Areal Density BPMR

Lin M. M. Myint<sup>1</sup>, Chanon Warisarn<sup>2</sup>, and Pornchai Supnithi<sup>3</sup>

<sup>1</sup>School of Science and Technology, Shinawatra University, Pathumthani 12160, Thailand

<sup>2</sup>College of Advanced Manufacturing Innovation, King Mongkut's Institute of Technology Ladkrabang, Bangkok 10520, Thailand

<sup>3</sup>Faculty of Engineering, King Mongkut's Institute of Technology Ladkrabang, Bangkok 10520, Thailand

For the high areal density bit patterned media recording (BPMR) systems, various multi-track equalization and detection techniques were proposed to mitigate the inter-track interference (ITI) so as to recover recorded data from the detecting tracks efficiently, but most works rarely aim to recover the recorded data on the sidetracks concurrently. As anticipation of that the readback signal has the intense contributions from the sidetracks due to high areal density, in this paper, we attempt to estimate the recorded data from the sidetracks as well as the detecting tracks by a multi-track joint detector that processes multi-track readback signals jointly in a single detector. To avoid the high complexity, which is the main shortfall in realizing the multi-track joint detector, we propose to employ a multi-track joint detector with a reduced complexity trellis for multi-head multi-track systems, in particular, four-head four-track (4H4T) BPMR system. To reduce the number of states in the trellis, the signals are equalized to 2-D generalized partial response targets whose cornered ITI coefficients are set to zero. The parallel branches are also incorporated in the trellis to estimate the data on the sidetracks. Moreover, we propose a two-head four-track (2H4T) system which generates the estimates of the recorded data on the four tracks by processing the signals from only two tracks. According to the simulation results, the proposed detector performs well on the data estimation of the detecting tracks as well as the sidetracks in both 4H4T and 2H4T systems.

**Index Terms**—Bit-patterned media recording (BPMR), equalization, multi-head multi-track (MHMT), multi-track joint detector.

## I. INTRODUCTION

INTER-TRACK interference (ITI) is one of the dominant challenges to be tackled in the ultra-high areal density magnetic recording systems such as bit patterned media recording (BPMR) system. In BPMR, each information bit is recorded on an isolated magnetic island which is composed of a single grain (or a few islands) so as to overcome the superparamagnetic limit [1]. However, increasing the areal density will inevitably lead to the narrow bit periods and track pitches, thereby resulting in more severe inter-symbol interference (ISI) and ITI effects in the readback signals. The ITI effects can severely degrade the performance of a conventional single track equalization and detection which are devised to handle the ISI alone. In overcoming the ITI obstacles in the high areal density magnetic recording systems, the advantages of multi-head multi-track (MHMT) systems with array readers are discussed in [2]–[6]. In those MHMT systems, the multi-track joint equalizer usually handles the ITI effects on the readback signals with the aid of the signals from the sidetracks before sending to a 2-D detector. Instead of the single-track detector, multi-track detection approaches were also proposed to mitigate the ITI by exchanging the ITI information between the multiple detectors and the decoders in [7] and [8]. The schemes achieve the performance gains by processing the ITI information from other detectors or the decoders.

Multi-track joint detectors have recently attracted much attention in the literature for combating the ITI problems [9]–[13]. Unlike single-track detectors, this detector processes multi-track signals jointly and estimates the recorded bits on multiple tracks using the array readers; hence, the ITI effects among the detecting tracks can be internally handled using a combined trellis which is constructed by integrating all tracks involved including the sidetracks. Zheng *et al.* [9] investigated the performance of multi-track joint detector and showed that the higher performance gains can be achieved by processing more readback signals concurrently. However, the complexity of this detector is prohibitively high for implementation even for the small number of tracks involved. To reduce the complexity, Fan *et al.* [11] proposed a reduced-state sequence estimation and analyzed its performance with different configurations of MHMT. In [12], the complexity reduction was attempted with the help of the 1-D equalizers and 2-D generalized partial response (GPR) targets. This proposed method considers the readback signals from the detecting tracks only after mitigating the ITI from the sidetracks by the equalizers.

Conventionally, most MHMT systems aim to control or mitigate the ITI effects using the multi-track joint equalization and detector, but most works rarely attempt to recover the recorded data on the sidetracks while processing the readback signals because of the assumption that the contributions from the sidetracks are too small to be recovered. However, we can anticipate that the ITI contributions from the sidetracks on the readback signals become more intense when the areal density of BPMR continues to increase. Therefore, it is possible to recover the recorded data on the sidetracks using a robust multi-track joint detector and utilize those estimates in the

Manuscript received March 14, 2018; revised April 27, 2018; accepted May 14, 2018. Date of publication June 8, 2018; date of current version October 17, 2018. Corresponding author: L. M. M. Myint (e-mail: lin@siu.ac.th).

Color versions of one or more of the figures in this paper are available online at <http://ieeexplore.ieee.org>.

Digital Object Identifier 10.1109/TMAG.2018.2839682

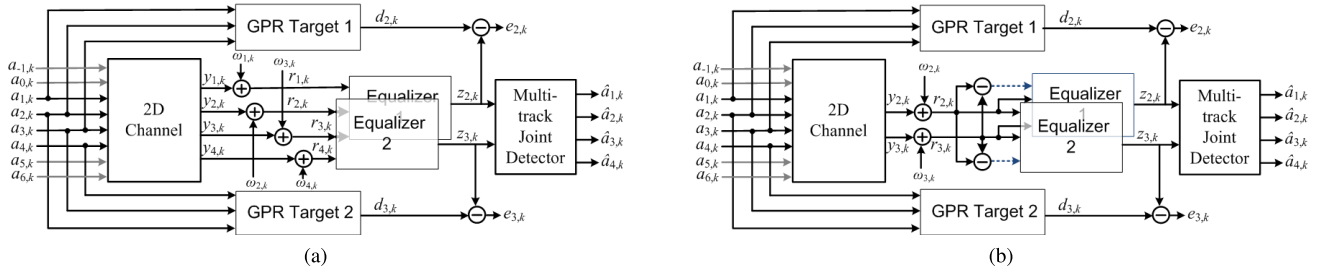


Fig. 1. Models of BPMR's MHMT system with the multi-track joint equalization and the proposed multi-track joint detector. (a) 4H4T system. (b) 2H4T system.

further decoding process so that the throughput of the MHMT system can be increased [14]. However, the complexity of the detector is needed to reduce the practically implementable levels.

Therefore, in this paper, we propose a multi-track joint detector using a reduced complexity trellis to recover the recorded data bits from the detecting tracks as well as the sidetracks for the high areal density BPMR with MHMT systems, particularly a four-head four-track (4H4T) system. In this system, the 2-D equalizers equalize the readback signals to 2-D GPR targets in which some ITI coefficients are set to zero in order to reduce the number of states in the trellis. The equalizers and targets are concurrently designed by minimizing the mean squared error (MSE) similar to [3], [6], and [15]. The parallel branches are incorporated into the trellis to estimate the data on sidetracks. With anticipation that each readback signal contains the substantial contributions from the side-tracks, the proposed system can generate the estimated data from the sidetracks with the acceptable reliabilities. Moreover, we propose a two-head four-track (2H4T) system using the proposed detector. Although it receives the signals from two detecting tracks only, the data on sidetracks can be estimated.

## II. BPMRS CHANNEL MODEL

In this paper, we consider a channel model of BPMR system from [13]. The readback signal  $r_{l,k}$  from the  $k$ th magnetic island along the  $l$ th track is expressed as

$$r_{l,k} = \sum_{m=-M}^M \sum_{n=-N}^N h(m,n) a_{l-m,k-n} + \omega_{l,k} \quad (1)$$

where  $a_{l,k} \in \{-1, 1\}$  is the recorded bit from the  $k$ th island along the  $l$ th track,  $h(m,n)$ s are the coefficients of a discrete-time 2-D Gaussian pulse channel response,  $2M+1$  and  $2N+1$  are the number of coefficients in the channel, and  $\omega_{l,k}$  is an additive white Gaussian noise (AWGN) with a standard deviation  $\sigma_l$ . The discrete-time 2-D Gaussian pulse response in [13] is generated by

$$h(m,n) = A \exp \left[ -a \left( \frac{nT_x}{PW_{50x}} \right)^2 - b \left( \frac{mT_z}{PW_{50z}} \right)^2 \right] \quad (2)$$

where  $A$  is the amplitude of the pulse response,  $T_x$  and  $T_z$  are the bit period and the track pitch, respectively, and  $PW_{50x}$  and  $PW_{50z}$  are the widths of the pulse response at its half maximum (PW50) in the along-track and the across-track

directions. Then,  $a$  and  $b$  are the fitting parameters related to the geometry of the magnetic bit island and the magnetic reader.

## III. MULTI-HEAD MULTI-TRACK SYSTEM

To estimate the recorded bits from the detecting tracks, most MHMT systems need the readback signals from both the detecting tracks and the sidetracks because the equalization system utilizes the sidetrack's signals to control the ITI effects on the readback signals. Therefore, the number of estimating tracks by the MHMT systems is usually fewer than the number of tracks needed by the equalization. In contrast, we consider two MHMT systems: 4H4T system and 2H4T system, in this paper. In both systems, we employ a multi-track joint equalization method to equalize the readback signals to the GPR targets with the ITI constraints.

The 4H4T system that receives the signals from the four tracks and generates the estimates of those four tracks is shown in Fig. 1(a). In this system, four readers sense the readback signals,  $r_{l,k}$ , from four consecutive tracks: the two detecting tracks, i.e., track 2 and track 3, and the two sidetracks, i.e., track 1 and track 4. Assuming that each readback signal is affected by the ITI effects from the two adjacent tracks above and two tracks below the middle track, the signal,  $r_{2,k}$ , has the contributions mainly from the bit on track 2,  $a_{2,k}$ , as well as partially from the bits on tracks 1 and 3,  $a_{1,k}$  and  $a_{3,k}$  (insignificantly from tracks 0 and 4). Similarly, the readback signal,  $r_{3,k}$ , contains the contributions from the bits on tracks 2, 3, and 4, i.e.,  $a_{2,k}$ ,  $a_{3,k}$ , and  $a_{4,k}$ . In here, it is important to note that the signals from the sidetracks are used only in the equalizers, not in the detector. The 2-D equalizer  $F_1$  equalizes the signal  $r_{2,k}$  according to the 2-D GPR target  $G_1$  using the signals  $r_{1,k}$  and  $r_{3,k}$  as its sidetracks and then generates the equalized signal  $d_{2,k}$ . Similarly, the 2-D equalizer  $F_2$  generates the equalized signal  $d_{3,k}$  by processing the signals,  $r_{2,k}$ ,  $r_{3,k}$ , and  $r_{4,k}$ . Thereafter, the multi-track joint detector recovers the recorded data bits from all four tracks, from 1 to 4, by processing these two equalized signals.

As a simplified MHMT system, we also devise a 2H4T system that receives the signals from two tracks and estimates the recorded bits on four tracks, as illustrated in Fig. 1(b). In the system, the equalizers receive the readback signals  $r_{2,k}$  and  $r_{3,k}$  from the two readers but no signals from the sidetracks. Since the equalizers equalize the readback signals  $r_{2,k}$  and  $r_{3,k}$  according to the respective 2-D GPR target

that intends to include the ITI coefficients of the sidetracks, i.e., track 1 or track 4 as to be discussed in Section IV, the equalizers still need the third input signal that include the information of the recorded bits on the sidetrack 1 or 4. Therefore, we generate a new signal sequence which is the difference between two readback signals, i.e.,  $r_{2,k}$  and  $r_{3,k}$ , and it is fed to both equalizers to help the equalizing process in this 2H4T system. Then, the multi-track joint detector estimates the recorded bits from all four tracks.

#### IV. MULTI-TRACK JOINT EQUALIZATION

In both MHT systems, we employ two multi-track joint equalizers with a size of  $3 \times (2L+1)$  to equalize the respective readback signals according to the 2-D GPR targets with a size of  $3 \times 3$ . The equalizer matrix  $\mathbf{F}_I$  and the GPR target matrix  $\mathbf{G}_I$  are defined as

$$\mathbf{F}_I = \begin{bmatrix} \mathbf{f}_{-1} \\ \mathbf{f}_0 \\ \mathbf{f}_1 \end{bmatrix} = \begin{bmatrix} f_{-1,-L} & \cdots & f_{-1,0} & \cdots & f_{-1,L} \\ f_{0,-L} & \cdots & f_{0,0} & \cdots & f_{0,L} \\ f_{1,-L} & \cdots & f_{1,0} & \cdots & f_{1,L} \end{bmatrix} \quad (3)$$

and

$$\mathbf{G}_I = \begin{bmatrix} \mathbf{g}_{-1} \\ \mathbf{g}_0 \\ \mathbf{g}_1 \end{bmatrix} = \begin{bmatrix} g_{-1,-1} & g_{-1,0} & g_{-1,1} \\ g_{0,-1} & g_{0,0} & g_{0,1} \\ g_{1,-1} & g_{1,0} & g_{1,1} \end{bmatrix} \quad (4)$$

where  $I \in \{1, 2\}$  is the index of the equalizer and the target related to the detecting tracks (tracks 2 and 3), respectively. For the proposed detector, we impose the constraints on the targets. Particularly, the coefficients of  $g_{-1,-1}$  and  $g_{-1,1}$  in  $\mathbf{G}_1$ , and  $g_{1,-1}$  and  $g_{1,1}$  in  $\mathbf{G}_2$  are set to 0 (to reduce the complexity of trellis) and coefficient  $g_{0,0}$  in both targets to 1. Each pair of 2-D equalizer  $\mathbf{F}_I$  and 2-D target  $\mathbf{G}_I$  are designed by minimizing the MSE. The MSE is expressed with the error sequence  $e_{l,k}$ , i.e.,

$$\begin{aligned} E\{e_{l,k}^2\} &= E\{(z_{l,k} - d_{l,k})^2\}, \text{ where } l \in \{2, 3\} \\ &= E\left\{\left(\sum_{m=-1}^1 \sum_{n=-L}^L f_{m,n} r_{l+m,k-n} - \sum_{m=-1}^1 \sum_{n=-1}^1 g_{m,n} a_{l+m,k-n}\right)^2\right\} \end{aligned} \quad (5)$$

where  $E\{\cdot\}$  is the expectation,  $z_{l,k}$  is the equalized signal sequence, and  $d_{l,k}$  is the desired signal sequence or the output of the target.  $f_{m,n}$  and  $g_{m,n}$  represent the coefficients of the equalizer  $\mathbf{F}_I$  in (3) and the target  $\mathbf{G}_I$  in (4). By minimizing the MSE in (5), similar to [3], [6], and [15], each pair of the equalizer and the target can be obtained from

$$\bar{\mathbf{g}}_I = (\mathbf{R}_a - \mathbf{R}_{ra}^T \mathbf{R}_r \mathbf{R}_{ra})^{-1} \mathbf{E}_I \lambda_I \quad (6)$$

$$\bar{\mathbf{f}}_I = \mathbf{R}_r^{-1} \mathbf{R}_{ra} \bar{\mathbf{g}}_I \quad (7)$$

where  $\bar{\mathbf{g}}_I = [\mathbf{g}_{-1}, \mathbf{g}_0, \mathbf{g}_1]^T$  and  $\bar{\mathbf{f}}_I = [\mathbf{f}_{-1}, \mathbf{f}_0, \mathbf{f}_1]^T$  are the column vectors by rearranging the matrices in (3) and (4),  $\mathbf{R}_r$  and  $\mathbf{R}_a$  are the auto-correlation matrices of the readback signal sequences and the recorded bit sequences on the three tracks involved, respectively, and  $\mathbf{R}_{ra}$  is a cross correlation

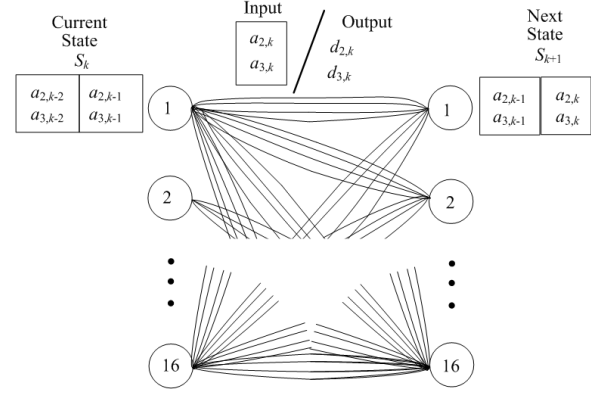


Fig. 2. Reduced complexity trellis for the multi-track joint detector.

matrix of the readback signal sequences and the recorded bit sequences.  $\lambda_I$  is a vector with the Lagrange multipliers, i.e.,

$$\lambda_I = [\mathbf{E}_I^T (\mathbf{R}_a - \mathbf{R}_{ra}^T \mathbf{R}_r \mathbf{R}_{ra})^{-1}]^{-1} \mathbf{c}_I \quad (8)$$

where  $\mathbf{E}_I$  and  $\mathbf{c}_I$  are the vectors which impose the above constraints of  $\mathbf{G}_I$  so that  $\mathbf{E}_I \bar{\mathbf{g}}_I = \mathbf{c}_I$ .

#### V. MULTI-TRACK JOINT DETECTOR WITH REDUCED COMPLEXITY TRELLIS

In this paper, we propose a multi-track joint 2-D detector using a reduced complexity trellis that can recover the recorded bits from the detecting tracks and sidetracks by processing two equalized signals from the detecting tracks 2 and 3. For the trellis structure, an input symbol consists of the bits from the detecting tracks, i.e.,  $a_{2,k}$  and  $a_{3,k}$ . Since there are two delay taps in the GPR targets in (4), there are  $4 \times 4 = 16$  states in the trellis. Given two bits in each input symbol, each state is connected to next four states at each state transition. The recorded bits from sidetracks are integrated into the trellis as parallel branches, as shown in Fig. 2. As discussed in Section IV, the cornered ITI coefficients in the targets are set to zero; hence, only the recorded bits from the sidetracks are considered. With all the possible combinations of  $(a_{1,k-1}, a_{4,k-1}) \in \{(-1, -1), (-1, 1), (1, -1), (1, 1)\}$ , there are four parallel branches at each state transition. In this paper, we consider only AWGN noise in the channel. Thus, using the log-likelihood method in [16], the computation of the branch metric for each parallel branch at each state transition can be simplified as

$$\mu(\zeta_k) = (z_{2,k} - d_2(\zeta_k))^2 + (z_{3,k} - d_3(\zeta_k))^2 \quad (9)$$

where  $z_{l,k}$  and  $d_l(\zeta_k)$  are the equalized signal and the desired signal with  $l \in \{2, 3\}$ , and  $\zeta_k$  represents the state transition between the current state  $S_k$  at time  $k$  and the next state  $S_{k+1}$  at time  $k+1$ . With the coefficients of two GPR targets and the values of  $a_{1,k-1}$  and  $a_{4,k-1}$  of the given parallel branches, the desired signals are calculated as

$$d_2(\zeta_k) = \sum_{m=0}^1 \sum_{n=-1}^1 g_{m,n} a_{2+m,k-n} + g_{-1,0} a_{1,k-1} \quad (10)$$

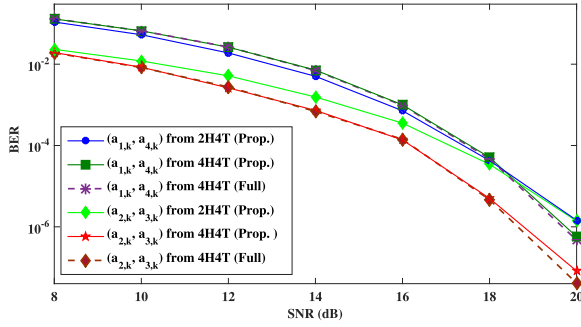


Fig. 3. Performance comparison of 4H4T system and 2H4T system using the proposed detector and the full-fledged detector for the BPMR system at the areal density of 4 Tb/in<sup>2</sup>.

and

$$d_3(\zeta_k) = \sum_{m=-1}^0 \sum_{n=-1}^1 g_{m,n} a_{3+m,k-n} + g_{1,0} a_{4,k-1}. \quad (11)$$

While the Viterbi algorithm finds the survivor path for each state at every state transition  $\zeta_k$ , it computes the path metrics for all parallel branches, and then selects the state transition which includes the parallel branch with the minimum path metric as a survivor. Thus, for each state at every state transition, the system needs to store the survivor state transition, its selected parallel branch and its path metric. After achieving the path with the minimum metric along the received signal sequence, the estimated recorded bits  $\hat{a}_{2,k}$  and  $\hat{a}_{3,k}$  from the detecting tracks are generated based on the survivor state transition along the path, and the estimated recorded bits  $\hat{a}_{1,k}$  and  $\hat{a}_{4,k}$  from the sidetracks are generated based on the selected parallel branch.

## VI. SIMULATION RESULTS AND DISCUSSION

In this paper, we consider a BPMR system with the areal density of 4 Tb/in<sup>2</sup> from [13], where the ITI effect is significantly severe so that the proposed detector is expected to be able to estimate the sidetrack's data. The size of islands is 7 nm × 7 nm, and the configuration of the reader is 21 nm × 21 nm × 3 nm. Both the bit period and the track pitch are 12.7 nm, and other parameters in (2) are  $A = 1$ ,  $a = 0.35$ ,  $b = 0.4$ ,  $PW_{50x} = 4.2$  nm, and  $PW_{50z} = 8.4$  nm. Setting  $M = 2$  and  $N = 1$ , the 2-D channel response matrix with a size of  $5 \times 3$  is

$$\mathbf{H} = \begin{bmatrix} 0.001 & 0.026 & 0.001 \\ 0.016 & 0.401 & 0.016 \\ 0.041 & 1 & 0.041 \\ 0.016 & 0.401 & 0.016 \\ 0.001 & 0.026 & 0.001 \end{bmatrix}. \quad (12)$$

From (12), the intermediate adjacent ITI coefficients are obviously higher than the ISI coefficients. The SNR is defined as  $\text{SNR} = 10\log_{10}(1/\sigma_l^2)$  where  $\sigma_l^2$  is the variance. The equalizers with a size of  $3 \times 11$  (by setting  $L = 5$ ) and the targets are designed using the MMSE technique at  $\text{SNR} = 18$  dB.

For performance comparison, we consider a multi-track joint detector with the full-fledged trellis from [9] for the 4H4T

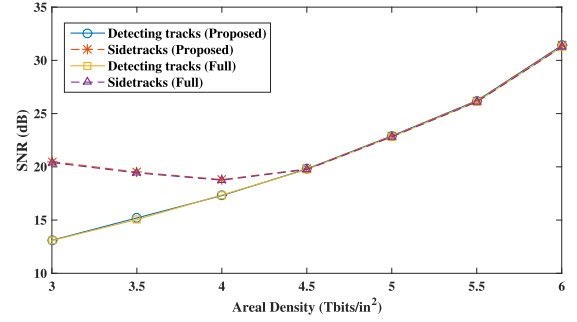


Fig. 4. SNR required by the proposed and full-fledged detectors in the 4H4T systems to achieve  $\text{BER} = 10^{-5}$  for the range of areal density.

system. In this trellis, the state is defined with the data bits from the detecting tracks and the sidetracks together, resulting in 256 states and 16 branches at each state. In the numerical simulations, we compute the bit error rates (BERs) of the detecting tracks with the sequences  $\hat{a}_{2,k}$  and  $\hat{a}_{3,k}$  together and, similarly, the BERs of the sidetracks with the sequences  $\hat{a}_{1,k}$  and  $\hat{a}_{4,k}$ . The performance comparison of the proposed detector in the 4H4T system and the 2H4T system to the full-fledged detector of the 4H4T system is shown in Fig. 3. For the estimated data from the detecting tracks and the sidetracks, the performances of proposed detector and the full-fledged detector in the 4H4T system are comparable. However, the full-fledged detector outperforms the proposed detector for the detecting tracks at high SNR levels. The performance of 2H4T system using the proposed detector is significantly inferior to the 4H4T systems, particularly, at high SNR levels because the 2H4T system receives only two readback signals. For the sidetrack's data estimation, the 2H4T system performs similar to the 4H4T systems until  $\text{SNR} = 18.3$  dB. The SNRs (dB) required by the proposed and full-fledged detectors in the 4H4T systems to achieve  $\text{BER} = 10^{-5}$  at the areal densities from 3 to 6 Tb/in<sup>2</sup> are studied in Fig. 4. The proposed detector can perform as well as the full-fledged detector. From 4.5 Tb/in<sup>2</sup>, the performance of detecting tracks and sidetracks are very comparable due to the high ITI levels in the channel.

## VII. CONCLUSION

In this paper, we propose a multi-track joint detector using a reduced complexity trellis to recover the recorded data bits on both the detecting tracks and the sidetracks with the help of multi-track joint equalization technique for the high areal density BPMR system. In the trellis, the recorded bits on the sidetracks are integrated as the parallel branches at each state transition. When each readback signal contains the substantial contributions from the sidetracks, the proposed system can generate the estimated data from the sidetracks with the acceptable reliabilities. The simulation results show that the proposed detector with the 4H4T system can recover the data from the sidetracks as well as the detecting tracks. There is a performance gap between the data estimation from the detecting tracks and the sidetracks, but it can be reduced further by error correction codes. These detected data on the sidetracks can be used in detecting the track during the next scan using an iterative process. Moreover, we devised and studied the proposed detector with the 2H4T system as a



simplified MHMT. The results show that there is a possibility to recover the data from the sidetracks with the proposed detector with some penalty even though the equalization system receives only the readback signals from the detecting tracks alone.

#### ACKNOWLEDGMENT

This work was supported in part by the Office of the Higher Education Commission Thailand and in part by the Thailand Research Fund under Grant MRG6080110.

#### REFERENCES

- [1] P. W. Nutter, I. T. Ntorkas, and B. K. Middleton, "An investigation of the effects of media characteristics on read channel performance for patterned media storage," *IEEE Trans. Magn.*, vol. 41, no. 11, pp. 4327–4334, Nov. 2005.
- [2] G. Mathew, E. Hwang, J. Park, G. Garfunkel, and D. Hu, "Capacity advantage of array-reader-based magnetic recording (ARMR) for next generation hard disk drives," *IEEE Trans. Magn.*, vol. 50, no. 3, pp. 155–161, Mar. 2014.
- [3] S. Nabavi and B. V. K. V. Kumar, "Two-dimensional generalized partial response equalizer for bit-patterned media," in *Proc. IEEE Int. Conf. Commun.*, Glasgow, U.K., Jun. 2007, pp. 6249–6254.
- [4] S. Nabavi, B. V. K. V. Kumar, and J.-G. Zhu, "Modifying Viterbi algorithm to mitigate intertrack interference in bit-patterned media," *IEEE Trans. Magn.*, vol. 43, no. 6, pp. 2274–2276, Jun. 2007.
- [5] S. Karakulak, P. H. Siegel, J. K. Wolf, and H. N. Bertram, "Joint-track equalization and detection for bit patterned media recording," *IEEE Trans. Magn.*, vol. 46, no. 9, pp. 3639–3647, Sep. 2010.
- [6] W. Chang and J. R. Cruz, "Inter-track interference mitigation for bit-patterned magnetic recording," *IEEE Trans. Magn.*, vol. 46, no. 11, pp. 3899–3908, Nov. 2010.
- [7] L. M. M. Myint, P. Supnithi, and P. Tantaswadi, "An inter-track interference mitigation technique using partial ITI estimation in patterned media storage," *IEEE Trans. Magn.*, vol. 45, no. 10, pp. 3691–3694, Oct. 2009.
- [8] G. Han, Y. L. Guan, K. Cai, and K. S. Chan, "Asymmetric iterative multi-track detection for 2-D non-binary LDPC-coded magnetic recording," *IEEE Trans. Magn.*, vol. 49, no. 10, pp. 5215–5221, Oct. 2013.
- [9] N. Zheng, K. S. Venkataraman, A. Kavcic, and T. Zhang, "A study of multitrack joint 2-D signal detection performance and implementation cost for shingled magnetic recording," *IEEE Trans. Magn.*, vol. 50, no. 6, Jun. 2014, Art. no. 3100906.
- [10] H. Saito, "Signal-processing schemes for multi-track recording and simultaneous detection using high areal density bit-patterned media magnetic recording," *IEEE Trans. Magn.*, vol. 51, no. 11, Nov. 2015, Art. no. 3101404.
- [11] B. Fan, H. K. Thapar, and P. H. Siegel, "Multihead multitrack detection for next generation magnetic recording, part I: Weighted sum subtract joint detection with ITI estimation," *IEEE Trans. Commun.*, vol. 65, no. 4, pp. 1635–1648, Apr. 2017.
- [12] L. M. Myint and C. Warisarn, "Reduced complexity of multi-track joint 2-D Viterbi detectors for bit-patterned media recording channel," *AIP Adv.*, vol. 7, no. 5, p. 056502, 2017.
- [13] Y. Wang and B. V. K. V. Kumar, "Improved multitrack detection with hybrid 2-D equalizer and modified Viterbi detector," *IEEE Trans. Magn.*, vol. 53, no. 10, Oct. 2017, Art. no. 3000710.
- [14] L. M. Myint and P. Supnithi, "Sidetrack data estimation using multi-track joint 2-D Viterbi detector," in *Proc. ECTI-CON Thailand*, Jul. 2018.
- [15] J. Moon and W. Zeng, "Equalization for maximum likelihood detectors," *IEEE Trans. Magn.*, vol. 31, no. 2, pp. 1083–1088, Mar. 1995.
- [16] B. Vucetic and J. Yuan, *Turbo Codes: Principles and Applications*, 2nd ed. Norwell, MA, USA: Kluwer, 2000.



# Reduced Complexity Multi-track Joint Equalization and Detection of High Areal Density Magnetic Recording

[View Session Detail](#)

Presentation Number: HV-15

Lin Myint<sup>\*1</sup>, Chanon Warisarn<sup>2</sup>, Pornchai Supnithi<sup>3</sup>

<sup>1</sup>School of Science and Technology, Shinawatra University, Thailand, Pathum Thani, Pathum Thani, Thailand;

<sup>2</sup>College of Advanced Manufacturing Innovation, King Mongkut's Institute of Technology Ladkrabang (KMITL), Bangkok, Bangkok, Thailand; <sup>3</sup>Telecommunications Engineering Department, King Mongkut's Institute of Technology Ladkrabang (KMITL), Bangkok, Bangkok, Thailand

**Digest Body:** In ultra-high areal density magnetic recording systems such as bit patterned media recording (BPMR) system, the width of a reader is expected to be relatively wider than the track pitch, thus, it will detect the magnetic field from the main track as well as those from the adjacent track which in turn resulting severe inter-track interference (ITI) effect on the readback signal. In the literature, multi-track joint detection techniques using array reader (AR) have been proposed to tackle ITI problem in future high areal density (AD) system [1-4] because it can provide a significant performance gain by processing multiple readback signals concurrently at the expense of high complexity. Most of researches focus on the data recovering from the single track or the number of tracks less than or equal to the number of readers while ITI effect from the sidetracks is alleviated. Considering the readback signal contains the significant contributions from the adjacent tracks, the system can generate the estimated data sequences not only from the main tracks but also from their adjacent tracks by employing the multi-track joint detection technique and AR. Therefore, in this paper, we propose a multi-track joint equalization and detection technique for a high AD magnetic recording system to recover the recorded data on four consecutive tracks (two tracks directly under the readers and two immediate sidetracks) by processing two readback signals from an array of two-reader. Given that each readback signal contains the substantial contributions from the sidetracks, we expect to achieve the estimated data from the sidetracks with the acceptable reliabilities for further decoding process. To reduce the detector's complexity, we also propose to use a multi-track Viterbi detector using a simplified trellis with parallel branches to recover data on the sidetracks.

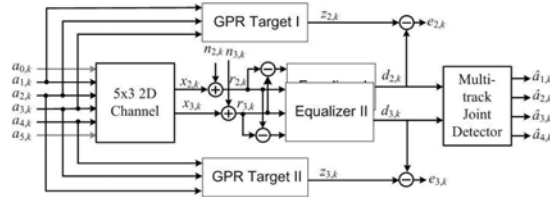
In the simulation model, we consider a discrete high areal density BPMR system with multi-track multi-head as shown in Fig. 1. The system is a two-head four-track system (2H4T) in which the data from four consecutive tracks, i.e.,  $a_{1,k}$ ,  $a_{2,k}$ ,  $a_{3,k}$  and  $a_{4,k}$  are recovered by processing the readback signals, i.e.,  $r_{2,k}$  and  $r_{3,k}$  from the array reader assuming that the centers of two head are aligned those of 2<sup>nd</sup> and 3<sup>rd</sup> track. To generate each readback signal, we use a two-dimensional (2-D) BPMR channel matrix with size of 5x3 and its coefficients are computed by a 2-D Gaussian pulse response using the parameters of areal density 4 Tb/in<sup>2</sup> from [4]. In the model, the readback signal,  $r_{2,k}$  has the contributions mainly from the data on the 2<sup>nd</sup> track,  $a_{2,k}$  as well as partially from the data on the 1<sup>st</sup> and 3<sup>rd</sup> tracks,  $a_{1,k}$  and  $a_{3,k}$  (insignificantly from the 0 and 4<sup>th</sup> track). Similarly, the readback signal,  $r_{3,k}$  contains the contributions from the data on the 2<sup>nd</sup>, 3<sup>rd</sup> and 4<sup>th</sup> track,  $a_{2,k}$ ,  $a_{3,k}$ ,  $a_{4,k}$ . In the equalization system, we employ two (2-D) equalizers, I and II, with size of 3x5 and two special (2-D) generalized partial response (GPR) targets, I and II, with size of 3x3,  $G_1 = [0, g_{1,2}, 0; g_{2,1}, g_{2,2}, g_{2,3}; g_{3,1}, g_{3,2}, g_{3,3}]$  and  $G_2 = [g_{1,1}, g_{1,2}, g_{1,3}; g_{2,1}, g_{2,2}, g_{2,3}; 0, g_{3,2}, 0]$  and they are designed using the minimum mean squared error (MMSE) method. Notice that some coefficients of target are set into zero aiming at reducing the trellis's complexity. The two readback signals are sent to the system. Assuming that the system is well synchronized and no frequency offset, the signal sequence is the difference between two readback signals, i.e.,  $r_{2,k}$  and  $r_{3,k}$ . Assuming the sequence  $\{r_{2,k} - r_{3,k}\}$  contains the contributions of the data on all four tracks, it is also fed to both equalizers as shown in Fig.1(a). Finally, the equalized signals  $d_{2,k}$  and  $d_{3,k}$  are processed in the multi-track joint Viterbi detector to generate the estimated data from four tracks. For the detector, the states and input symbols in trellis are considered with only the data,  $a_{2,k}$ ,  $a_{3,k}$ , thereby resulting only 16 states and 4 outgoing branches at each state. To recover the sidetracks' data,  $a_{1,k}$ ,  $a_{4,k}$  are considered as parallel branches between each state transition as shown in Fig. 2(a) [5]. In Viterbi algorithm, the branch with the minimum metric value among all parallel branches is selected as the survival path. To compare the proposed (2H4T) system, we consider a multi-track system employing a four-reader array (4H4T) in Fig.1(b). In this system, we consider a multi-track joint Viterbi detector employing a trellis with 256 states and 16

[Home](#)
[Schedule](#)
[Type](#)
[Search](#)
[More ..](#)

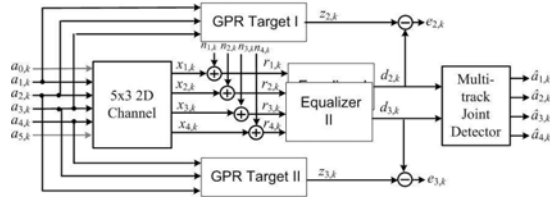
full-fledged system, but it can generate the estimated data sequence from the sidetracks with the acceptable reliabilities and then they can be improved by using a robust channel coding system.

Acknowledgement: This work was partly supported by the Thailand Research Fund (TRF) and Shinawatra University (SIU).

**References:** [1] G. Mathew, et al., "Capacity Advantage of Array-Reader-Based Magnetic Recording (ARMR) for Next Generation Hard Disk Drives," *IEEE Trans. Magn.*, vol. 50, no. 3, Mar. 2014.  
 [2] Y. Wang, B. Yuan and K. K. Parhi, "Improved BER Performance With Rotated Head Array and 2-D Detector in Two-Dimensional Magnetic Recording," in *IEEE Trans. Magn.*, vol. 52, no. 7, pp. 1-6, July 2016.  
 [3] J. R. Barry et al., "Optimization of Bit Geometry and Multi-Reader Geometry for Two-Dimensional Magnetic Recording," in *IEEE Trans. Magn.*, vol. 52, no. 2, pp. 1-7, Feb. 2016.  
 [4] Y. Wang and B. V. K. V. Kumar, "Multi-Track Joint Detection for Shingled Magnetic Recording on Bit Patterned Media With 2-D Sectors," in *IEEE Trans. Magn.*, vol. 52, no. 7, pp. 1-7, July 2016.  
 [5] S. Nabavi, B. V. K. V. Kumar and J. G. Zhu, "Modifying Viterbi Algorithm to Mitigate Intertrack Interference in Bit-Patterned Media," in *IEEE Trans. Magn.*, vol. 43, no. 6, pp. 2274-2276, June 2007.

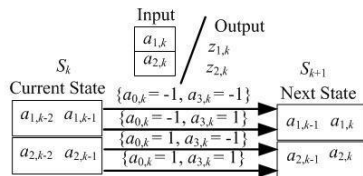


(a) 2H4T Multi-track Joint Detection System Model

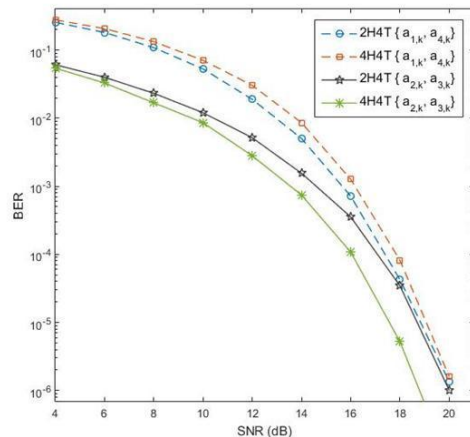


(b) 4H4T Multi-track Joint Detection System

Simulation Model,



(a) State transition for the proposed Trellis



(b) Performance comparison of Multi-track Joint Detections



# Sidetrack Data Estimation Using Multi-track Joint 2-D Viterbi Detector in Bit Patterned Media Storage

Lin Min Min Myint

*School of Science and Technology*

*Shinawatra University*

Pahtumthani 12160, Thailand

lin@siu.ac.th

Pornchai Supnithi

*Faculty of Engineering*

*King Mongkut's Institute of Technology Ladkrabang*

Bangkok 10520, Thailand

pornchai.su@kmitl.ac.th

**Abstract**—In the high areal density, bit patterned media recording (BPMR) system, the inter-track interference (ITI) effects become severe when the areal density is increased. In the literature, a multi-track joint 2-D detector with the aid of a multi-reader array technology is proposed to mitigate the ITI effect in BPMR systems because of its significant performance gains achieved by processing the multiple readback signals concurrently. In practice, the multi-track joint 2-D detector can estimate the recorded data from not only the detecting tracks, but also the sidetracks when the ITI effect is considerably high. Although the estimates of the data on the sidetracks are not as good as those on the detecting tracks, they can be applied in or improved by further coding process. In this work, we study the performance of a multi-track joint 2-D Viterbi detector for estimating the data on the sidetracks by adjusting the offset position of heads in the multi-head multi-track (MHMT) BPMR system. The detector recovers the recorded data on the detecting and sidetracks by processing the readback signals from the detecting tracks. We also investigate the performance changes due to the head offsets. The results show that the performance of detector for estimating the data on the sidetracks can be improved by adjusting the head offsets well.

**Index Terms**—Bit-patterned media recording (BPMR), inter-track interference (ITI), multi-track joint detection, Viterbi detector.

## I. INTRODUCTION

In the high areal density magnetic recordings system such as bit patterned media recording (BPMR) system, the bit period and track pitch of the BPMR will become narrower resulting in severe inter-symbol interference (ISI) and, in particular, inter-track interference (ITI) on the readback signals. Multi-track joint signal processing is one of the promising data recovery techniques to tackle ITI problem in the high areal density BPMR. To alleviate the ITI effects, a multi-track 2-D equalization was proposed in [1]–[3] and it processes the multi-track signals before a single track detector that is designed based on a 2-D generalized partial response (GPR) target. This method can provide higher performance gain than a conventional 1-D equalization. Alternatively, a multi-track detection was also proposed with the help of iterative signals processing in [4]. In this proposed method, multiple 1-D detectors process the multiple readback signals iteratively by exchanging the information with a low-density parity-check (LDPC) decoder to mitigate the ITI effects efficiently.

Given a conceived multi-head array technology, many researchers have studied the performance of multi-head multi-track (MHMT) system using a multi-track joint 2-D detector [5]–[7]. Unlike the conventional 2-D detector, the multi-track joint 2-D detector processes the readback signals from the multiple tracks concurrently, thereby achieving the significant performance gains at the expense of high complexity. Normally, the MHMT system aims to mitigate the ITI effects on the readback signals by processing the signals from the sidetracks so as to estimate the recorded data on the detecting tracks effectively. Most of earlier proposed MHMT systems usually do not attempt to recover the data from the sidetracks because of the assumption that the readback signals do not contain sufficient contributions of sidetracks to be recovered. In contrast, the researchers in [8] proposed an iterative multi-track detection concatenated with multiple decoders to recover the data from the sidetracks by processing just the signals from the detecting tracks, and proved that the proposed system can estimate the data on the sidetracks with a reasonable reliability. While the areal density of BPMR is increased further in the future, the intensity of ITI effects on the readback signal will be higher. Therefore, instead of attempting to mitigate the ITI, employing a robust 2-D data recovery system such as the multi-track joint 2-D detector can estimate the recorded data on the sidetracks from the readback signals while estimating the recorded data on the detecting track. As a result, the throughput capacity of MHMT system can be increased and the estimated data from the sidetracks can be used in further process.

In this work, we aim to study the performance of a multi-track joint 2-D Viterbi detector in conjunction with the multi-track 2-D equalization for estimating the recorded data on the sidetracks for the high areal density of BPMR system. In the system, the equalized signals from the detecting tracks are processed by the detector for estimating the recorded data on both the detecting tracks and the sidetracks concurrently. Due to the indistinguishable symbols, resulting the symmetric ITI effects, can degrade the performance of the detector, hence, we propose to set the head offsets into the direction of the sidetrack in the design of multi-head array. As a consequence, it can increase the contribution from the sidetrack on the readback signals. Then, we investigate the performance changes by

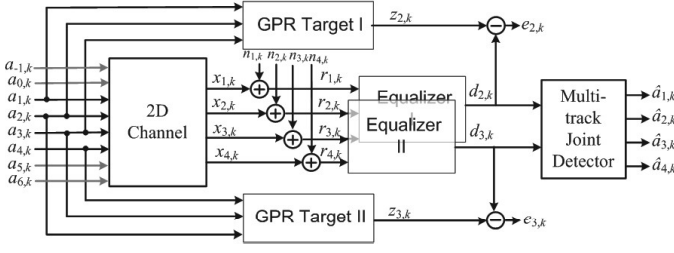


Fig. 1. The model of 4H4T BPMR channel with multi-track 2-D equalization and a multi-track joint 2-D detector.

that adjusting the head offset positions. The simulation results show that the data recovery performance of the sidetracks can be improved without significant losing the performance of the detecting tracks at the optimal head offset positions.

## II. BPMRS RECORDING CHANNEL MODEL

In this paper, we consider a discrete-time 2-D channel model of the high areal density BPMR system. Without considering the media noise and track mis-registration (TMR), the coefficients of discrete-time domain 2-D BPMR channel is computed using a Gaussian pulse response from [6], i.e.,

$$h(m, n) = A \exp \left[ -a \left( \frac{nT_x}{PW_{50x}} \right)^2 - b \left( \frac{mT_z + \tau_{off}}{PW_{50z}} \right)^2 \right], \quad (1)$$

where  $A$  is the amplitude of the pulse response,  $T_x$  and  $T_z$  are the bit period and the track pitch respectively,  $PW_{50x}$  and  $PW_{50z}$  are the width of the pulse response at its half maximum (PW50) in the along-track and the across-track directions, and  $\tau_{off}$  is the head offset position that is the offset distance between the center of head and that of track. Then,  $a$  and  $b$  are the fitting parameters depending on the geometry of the magnetic bit island and the magnetic reader element. Using (1), the readback signal,  $r_{l,k}$  from the  $k^{th}$  magnetic island along the  $l^{th}$  track is expressed as

$$r_{l,k} = \sum_{m=-M}^M \sum_{n=-N}^N h(m, n) a_{l-m, k-n} + n_{l,k}, \quad (2)$$

where  $a_{l,k}$  is the recorded data bit from the  $k^{th}$  island at the  $l^{th}$  track,  $h(m, n)$ s are the channel response coefficients from (1),  $2M$  and  $2N$  are the numbers of ITI and ISI coefficients, and  $n_{l,k}$  is an additive white Gaussian noise (AWGN) with a standard deviation  $\delta_l$ . We consider BPMR system with the areal density of 4 Tbits/in<sup>2</sup> from [6]. Therefore, the island size is 7 nm x 7 nm and the values of  $PW_{50x}$  and  $PW_{50z}$  are 4.2 nm and 8.4 nm, respectively. Using the same parameters of the head from [6], we generate a 5x3 channel response coefficient matrix setting by  $M = 2$  and  $N = 1$ . Therefore, each readback signal suffers the ITI effect from the two upper and two lower adjacent tracks. Without head offset, the generated 2-D channel response matrix with size of 5x3 using (1) is

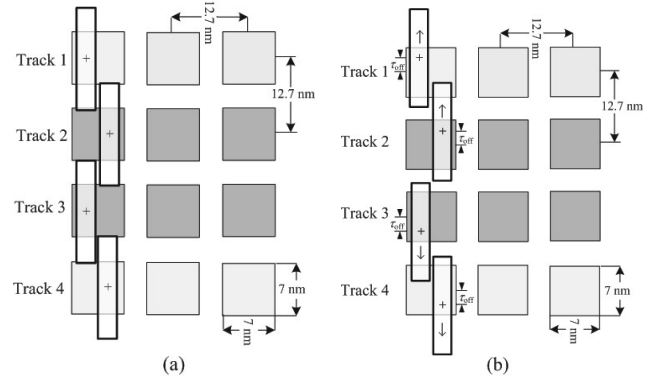


Fig. 2. The configuration of four heads (a) without head offset. (b) with head offset according to the direction of arrows.

$$\mathbf{H} = \begin{bmatrix} h_{-2,-1} & h_{-2,0} & h_{-2,1} \\ h_{-1,-1} & h_{-1,0} & h_{-1,1} \\ h_{0,-1} & h_{0,0} & h_{0,1} \\ h_{1,-1} & h_{1,0} & h_{1,1} \\ h_{2,-1} & h_{2,0} & h_{2,1} \end{bmatrix} = \begin{bmatrix} 0.001 & 0.026 & 0.001 \\ 0.016 & 0.401 & 0.016 \\ 0.041 & 1 & 0.041 \\ 0.016 & 0.401 & 0.016 \\ 0.001 & 0.026 & 0.001 \end{bmatrix}. \quad (3)$$

It is easy to note that, in the channel matrix the values of intermediate adjacent ITI coefficients are obviously higher than those of ISI coefficients, thus, the system is expected to recover the data from the sidetracks by processing the detecting tracks.

## III. 4H4T EQUALIZATION AND DETECTION SYSTEM

In this work, we consider a four-head four-track (4H4T) read channel of the BPMR system with an array of four heads as shown in Fig. 1. In the system, an array of four heads detects the bit islands on four adjacent tracks,  $l \in \{1, 2, 3, 4\}$  concurrently as depicted in Fig.1, and then generates four readback signals, i.e.,  $r_{1,k}, r_{2,k}, r_{3,k}$  and  $r_{4,k}$  using (2). The configurations of the head array with and without the head offset are shown in Fig.2. In Fig.2(a), the center of each head is aligned with that of the tracks when the value of  $\tau_{off}$  is zero. In this paper, we propose to shift the heads on the tracks 1 and 2 into upward direction and the heads on the tracks 3 and 4 in downward direction by the value of  $\tau_{off}$  as illustrated by the arrows in Fig.2(b). It results to higher ITIs from the sidetracks, but less from other detecting track onto the signals  $r_{2,k}$  and  $r_{3,k}$ . The negative value of  $\tau_{off}$  means the reverse offset movement of heads so that the readback signals will have more ITI from other detecting tracks but less from the sidetracks.

In the system, the readback signals are sent to the respective 2-D equalizer as depicted in Fig.1. The Equalizer I generates the equalized signal  $d_{2,k}$  by processing the signals,  $r_{1,k}, r_{2,k}$  and  $r_{3,k}$ , and the Equalizer II generates  $d_{3,k}$  by processing the signals,  $r_{2,k}, r_{3,k}$  and  $r_{4,k}$ . Thereafter, two equalized signals are fed to a multi-track joint 2-D detector to generate the estimated recorded data sequences,  $\{\hat{a}_{1,k}\}, \{\hat{a}_{2,k}\}, \{\hat{a}_{3,k}\}$  and

$\{\hat{a}_{4,k}\}$ . Here, notice that even though all readback signals are fed into the two equalizers, only the equalized readback signals,  $d_{2,k}$  and  $d_{3,k}$  are processed by the detector and the signals,  $r_{1,k}$  and  $r_{4,k}$  are just utilized to equalize the signals,  $r_{2,k}$  and  $r_{3,k}$  according to the 2-D generalized partial response (GPR) targets. Therefore, the tracks 2 and 3 are described as the detecting tracks and the tracks 1 and 4 as the sidetracks hereafter. For the detector, a full-fledged trellis is designed embedding the data bits on all four tracks (including the detecting tracks and the sidetracks) to be estimated. Since the detector processes only two equalized signals, the error rate in the sequences  $\{\hat{a}_{1,k}\}$  and  $\{\hat{a}_{4,k}\}$  are expected to be higher than that of the sequences  $\{\hat{a}_{2,k}\}$  and  $\{\hat{a}_{3,k}\}$ . However, we investigate the performance changes of each estimated sequences by adjusting the different head offset positions and search for the optimal positions.

#### A. Multi-track 2-D Equalizer and 2-D GPR Target Approach

In order to control the ITI effects on each readback signal, we consider two 2-D equalizers with the size of  $3 \times (2L+1)$  together with two 2-D GPR targets with the size of  $3 \times 3$ . The equalizer matrix  $\mathbf{F}_I$  and the target matrix  $\mathbf{G}_I$  are defined as

$$\mathbf{F}_I = \begin{bmatrix} f_{-1,-L} & \dots & f_{-1,0} & \dots & f_{-1,L} \\ f_{0,-L} & \dots & f_{0,0} & \dots & f_{0,L} \\ f_{1,-L} & \dots & f_{1,0} & \dots & f_{1,L} \end{bmatrix} \quad (4)$$

and

$$\mathbf{G}_I = \begin{bmatrix} g_{-1,-1} & g_{-1,0} & g_{-1,1} \\ g_{0,-1} & g_{0,0} & g_{0,1} \\ g_{1,-1} & g_{1,0} & g_{1,1} \end{bmatrix} \quad (5)$$

where  $I \in \{I, II\}$  is the index of the equalizer and the target. Each pair of 2-D equalizer  $\mathbf{F}_I$  and 2-D target  $\mathbf{G}_I$ , are designed based on MMSE technique using the respective error sequence  $e_{l,k}$ ,  $l \in \{2, 3\}$  is expressed by,

$$E\{e_{l,k}^2\} = E\{f_{l,k} \otimes r_{l,k} - g_{l,k} \otimes a_{l,k}\} \quad (6)$$

where  $E\{\cdot\}$  is the expectation,  $\otimes$  is a 2-D convolution.

#### B. Multi-track Joint 2-D Detector

In this work, the multi-track joint 2-D detector employs a full-fledged 2-D trellis constructed by considering the input bits from all four consecutive tracks (two detecting tracks and two sidetracks) to be estimated. Therefore, in the trellis, each input symbol is defined as  $\mathbf{a}_k = \{a_{1,k}, a_{2,k}, a_{3,k}, a_{4,k}\}$  and then each state is composed by two symbols based on the given 2-D GPR targets. As a result, the 2-D trellis contains  $2^{4 \times 2} = 256$  states and  $2^4 = 16$  incoming or outgoing branches at each state. Considering the log-likelihood method, the computation of branch metric for each transition of the trellis can be simplified as

$$\mu(\xi_k) = (d_{2,k} - z_2(\xi_k))^2 + (d_{3,k} - z_3(\xi_k))^2, \quad (7)$$

where  $d_{l,k}$  and  $z_l(\xi_k)$  are the equalized signal and target output of  $l \in \{2, 3\}$  tracks, and  $\xi_k$  represents the state

TABLE I  
ITI COEFFICIENTS IN (3) Vs. HEAD OFFSET

Head offset ( $\tau_{off}/T_z$ )	ITI coefficients [ $h_{-2,0}, h_{-1,0}, h_{0,0}, h_{1,0}, h_{2,0}$ ]
-0.15	[0.015, 0.305, 1, 0.527, 0.045]
-0.10	[0.018, 0.334, 1, 0.481, 0.037]
-0.05	[0.021, 0.365, 1, 0.439, 0.031]
0	[0.026, 0.401, 1, 0.401, 0.026]
0.05	[0.031, 0.439, 1, 0.365, 0.021]
0.10	[0.037, 0.481, 1, 0.334, 0.018]
0.15	[0.045, 0.527, 1, 0.305, 0.015]

transition between the current state  $S_k$  at time  $k$  and the next state  $S_{k+1}$  at time  $k+1$ . For branch metric in (7), each of target outputs is computed with the coefficients of the respective GPR target I and II. Using the Viterbi algorithm, the detector finally generates the estimated recorded bit sequences  $\{\hat{a}_{1,k}\}$ ,  $\{\hat{a}_{2,k}\}$ ,  $\{\hat{a}_{3,k}\}$  and  $\{\hat{a}_{4,k}\}$  by processing with the two equalized signals,  $d_{2,k}$  and  $d_{3,k}$  that contain the significant ITI contributions from tracks 1 and 4.

#### IV. SIMULATION RESULTS AND DISCUSSIONS

In this work, we consider a BPMR system with the areal density of 4 Tbits/in<sup>2</sup> from [6]. The signal-to-noise ratio (SNR) is defined as  $20\log(V_p/\delta_l)$ , where  $V_p = 1$  is the peak value of the readback signals and  $\delta_l$  is the standard deviation of AWGN. Each sector has 4096 bits. The equalizers and targets are designed with the known bit sequences at SNR = 18 dB using the MMSE technique.

Firstly, we observe the changes of the main ITI coefficients in the channel matrix in (3) generated by the head on the track 2 for the different head offset positions defined as the ratio of head offset position to the track pitch, i.e.,  $\tau_{off}/T_z$  in Table I. The value of the upper ITI coefficients will rise and the value of the lower ITI coefficients will fall when the value of ratio is changed from the negative values to the positive values. The changes of the ITI coefficients in the matrices generated by the heads on the tracks 1 will be in the same manner but those on the tracks 3 and 4 will generate inversely as they are offset in opposite direction. The readback signals will contain more ITI contributions from the sidetracks than the detecting tracks when the value of ratio is set to positive value; thus, it is expected that the system can estimate the recorded data on the sidetracks from the readback signals.

Then we investigate the data estimating performances of the 4H4T system using a multi-track joint 2-D detector from the detecting tracks, i.e., the tracks 2 and 3, and from the sidetracks, i.e., the tracks 1 and 4 at the SNR level of 18 dB for various head offset values and the simulation results are shown in Fig. 3. According to the results, the detector can improve the performance of estimating the data on the sidetracks without significantly deteriorating the performance of estimating data on the detecting tracks when the upper two

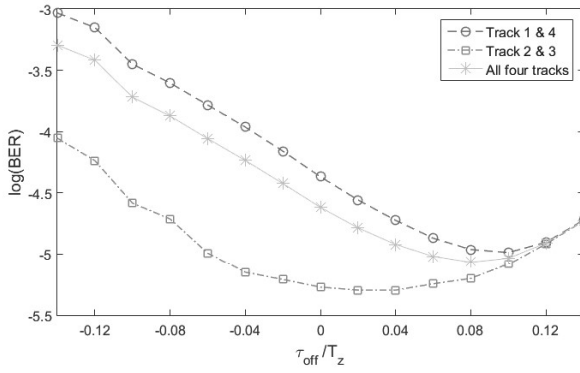


Fig. 3. Performance of the data estimates from the detecting tracks 2 & 3 and the sidetracks 1 & 4 according to various head offset values at SNR 18dB.

heads are offset away from the lower two heads because the detecting signals,  $r_{2,k}$  and  $r_{3,k}$  contain the more contributions from the sidetracks 1 and 4. After the ratio value of 0.08, their performance starts to decline again because of the significant performance degrading of the detecting tracks. However, when the upper pair of heads are adjusted closer to the lower pair of heads setting the negative values of the head offset ratio, the performance of the detector on all tracks is obviously degrading due to the less contributions from the sidetrack, but the higher ITI from other detecting track. Therefore, we assume the optimal performance of data estimating from all four tracks is achieved when each pair of heads are shifted away from other pair by about  $0.08 T_z$ .

Finally, the bit error rate (BER) performance of the 4H4T system with no head offset and with the head offset position of  $0.08 T_z$  are compared in Fig. 4. In the figure, the performance of the data estimation from the detecting tracks and the sidetracks are plotted separately. For the detecting tracks, the performance of the system with the head offset is insignificantly degraded compared to that of the system without the head offset because of the higher ITI effects. However, in contrast, the performance of the data estimating from the sidetracks by the system with head offset is better than the system with no head offset. The former can provide the performance gain of about 0.8dB at BER  $10^{-4}$ . This performance gain is achieved by the higher contributions from the sidetracks as well as the asymmetric GPR targets which are designed using the MMSE methods for the asymmetric channel matrix.

## V. CONCLUSION

We assume that the ITI contributions of the sidetracks on the readback signals become higher in the higher areal density of magnetic recording system. Based on this assumption, we expect that the robust detector with the help of multi-track signal processing can enable to estimate the recorded data from the sidetracks by processing the signals from the detecting tracks. In this paper, we study the performance of the recorded data estimation from the detecting tracks as well

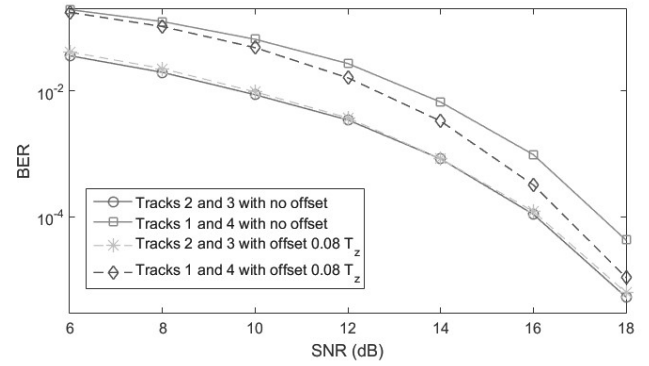


Fig. 4. The performance of estimating the data on the detecting tracks and the sidetracks with and without the optimal head offset positions.

as the sidetracks using a 4H4T BPMR system with multi-track 2-D equalization and a multi-track joint 2-D Viterbi detector. Moreover, we investigate the performance changes of the system by setting the various head offsets. Employing a high complexity trellis, the system can estimate the data on the detecting tracks and the sidetracks well by processing the readback signals from the detecting tracks only in the detector when the heads are offset optimally. There is a performance gap between the sidetracks and the detecting tracks; however, it can be narrowed down by further processing with the error control coding such as LDPC code in the system.

## ACKNOWLEDGMENT

This work was supported by the office of the Higher Education Commission Thailand and the Thailand Research Fund (TRF) under grant MRG6080110.

## REFERENCES

- [1] W. Chang and J. R. Cruz, "Inter-Track Interference Mitigation for Bit-Patterned Magnetic Recording," *IEEE Trans. Magn.*, vol. 46, no. 11, pp. 3899-3908, Nov. 2010.
- [2] S. Karakulak, P. H. Siegel, J. K. Wolf and H. N. Bertram, "Joint-Track Equalization and Detection for Bit Patterned Media Recording," *IEEE Trans. Magn.*, vol. 46, no. 9, pp. 3639-3647, Sept. 2010.
- [3] G. Mathew, E. Hwang, J. Park, G. Garfunkel and D. Hu, "Capacity Advantage of Array-Reader-Based Magnetic Recording (ARMR) for Next Generation Hard Disk Drives," *IEEE Trans. Magn.*, vol. 50, no. 3, pp. 155-161, March 2014.
- [4] L. Myint, P. Supnithi and P. Tantaswadi, "An Inter-Track Interference Mitigation Technique Using Partial ITI Estimation in Patterned Media Storage," *IEEE Trans. Magn.*, vol. 45, no. 10, pp. 3691-3694, Oct. 2009.
- [5] Zheng, K. S. Venkataraman, A. Kavcic and T. Zhang, "A Study of Multitrack Joint 2-D Signal Detection Performance and Implementation Cost for Shingled Magnetic Recording," *IEEE Trans. Magn.*, vol. 50, no. 6, pp. 1-6, June 2014.
- [6] Y. Wang and B. V. K. V. Kumar, "Improved Multitrack Detection With Hybrid 2-D Equalizer and Modified Viterbi Detector," *IEEE Trans. Magn.*, vol. 53, no. 10, pp. 1-10, Oct. 2017.
- [7] L. Myint and C. Warisarn, "Reduced complexity of multi-track joint 2-D Viterbi detectors for bit-patterned media recording channel," *AIP Advances*, Volume 7, Issue 5, id.056502, 2017.
- [8] G. Han, Y. L. Guan, K. Cai and K. S. Chan, "Asymmetric Iterative Multi-Track Detection for 2-D Non-Binary LDPC-Coded Magnetic Recording," *IEEE Trans. Magn.*, vol. 49, no. 10, pp. 5215-5221, Oct. 2013.

# Study of Detectors with Noise Predictor for High Areal Density BPMR Systems

Lin Min Min Myint  
School of Science and Technology  
Shinawatra University  
Pathumthani 12160, Thailand  
lin@siu.ac.th

Pornchai Supnithi  
Faculty of Engineering  
King Mongkut's Institute of Technology Ladkrabang  
Bangkok 10520, Thailand  
pornchai.su@kmitl.ac.th

**Abstract**—In this paper, we study the performance of Viterbi detector embedded with noise predictor for the 2-D interference channel of high areal density bit patterned media recording (BPMR) systems. The received signal at the input of detector is corrupted by the colored/correlated noise due to the partial response equalizer, and thus the noise whitening with noise predictor is required to improve the detector's performance. The noise predictor estimates the current noise sample based on the past noise samples using a noise prediction filter. The noise predictor is normally incorporated into the detector by extending the trellis, but it is impractical for the high complexity detector for the 2-D interference channels. Therefore, we design a detector embedded by a noise prediction technique without extending the trellis. In the proposed technique, the most likely noise samples are stored along the surviving path of the trellis when the branch metrics at state are computed and the survivor branch is selected in Viterbi algorithm. The proposed technique requires less number of memory and arithmetic operations at each state of the trellis compared to conventional technique. We consider both finite impulse response (FIR) filter and infinite impulse response (IIR) filter for the noise prediction filter. The simulation results show that the proposed noise prediction can improve the performance of detector, especially for the high areal density at 4 Tbit/in<sup>2</sup>.

**Index Terms**—Bit-patterned media recording, 2-D interference channel, noise prediction, Viterbi detector.

## I. INTRODUCTION

Bit patterned media recording (BPMR) technology is one of the candidates for future high-density magnetic recording storages to fulfill the exponential growth of big data generated by human and machines. In BPMR technology, the special magnetic media is fabricated with magnetic islands to record the information bits [1]. Each magnetic island is theoretically composed by a single grain to overcome the superparamagnetic limit and it is isolated by non-magnetic region to mitigate the nonlinear media noise. The superparamagnetic limit and the nonlinear media noise are the critical barriers for the conventional magnetic technologies to increase the recording density further. However, the readback signal from the BPMR media is corrupted by a two-dimensional (2-D) interference: inter-symbol interference (ISI) and inter-track interference (ITI) because of the narrow spacings between the recording bits and the tracks. In [2]–[4], 2-D generalized partial response

(GPR) equalizations using 1-D/2-D detectors were proposed to tackle the 2-D interference channel. Both maximum likelihood (ML) or Viterbi detector and maximum a Posteriori (MAP) detector are optimal for the channel corrupted by additive white Gaussian noise (AWGN) [5]. However, the performance of those detectors degrades to be suboptimal when the channel suffers the colored/correlated noise. When the data recovery system of magnetic recording employs a 2-D equalizer to shape the readback signal according to the 2-D GPR target before the detector, it correlates the corrupted AWGN noise to be a colored noise.

Therefore, it is required to whiten the noise before the detector for the performance improvement. In [6]–[8], the noise whitening techniques using a linear noise predictor were proposed for 1-D channel detector. In the techniques, the current noise sample is predicted from the past noise samples using a noise prediction filter (i.e. finite impulse response (FIR) filter or infinite impulse response (IIR) filter), and then the predicted noise sample is utilized in the branch metric calculation of the Viterbi algorithm. Conventionally, the noise predictor is incorporated by extending the trellis for the noise prediction with more possible input bits [7], [9], but it is impractical for the detector of the 2-D channel because of the high complexity. The noise prediction can also be done using the stored estimates of input bit along the surviving path like [8], [10] or of the feedback from the detector and the decoder in [11]. Even though these techniques do not need to extend the trellis, they are vulnerable to the error propagation because the prediction is based on the estimated information.

In this paper, we investigate the performance of Viterbi detectors embedded with a noise predictor for the 2-D interference channel of high areal density BPMR system. We propose a noise predictor that uses a prediction technique based on the recorded noise sample sequence along the surviving path of the trellis. During finding the surviving path in Viterbi algorithm, the error samples between the received signal sample and the desired output sample are computed for the branch metric calculation of all branch transitions toward the current state. If one of the branch transitions is selected as a part of the surviving path, the proposed technique stores the computed error sample as a estimated noise sample at the respective state for the noise prediction in further states. We consider

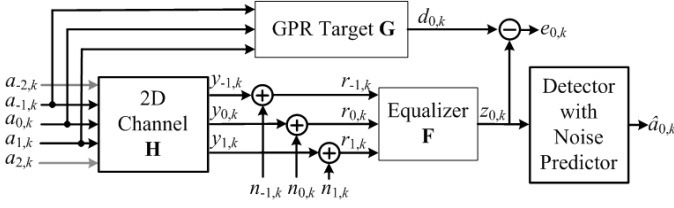


Fig. 1. The readback channel model of BPMR system.

a FIR filter as well as an IIR filter as a prediction filter in the study. Finally the detectors employed the proposed noise prediction are compared against the detectors with and without the noise predictor using extended trellis. The simulation result shows that the proposed noise techniques can provide the performance gain, especially for the BPMR system 4 Tbit/in<sup>2</sup>.

The rest of the paper is organized as follows. In Section II, we briefly describe a BPMR readback channel model. Section III explains the detector with noise predictor, the noise prediction filters and the proposed noise prediction technique. Simulation results are discussed in Section IV. Finally, Section V concludes this papers.

## II. BPMR'S READBACK CHANNEL MODEL

A block diagram of the BPMR's readback channel model is shown in Fig. 1. In the model,  $a_{l,k} \in \{-1, 1\}$  is the recorded bit on the  $k^{th}$  bit island along the  $l^{th}$  track. Without considering write errors and media noise, the BPMR's readback signal from the  $k^{th}$  bit island along the  $l^{th}$  track is defined as

$$r_{l,k} = \sum_{m=-M}^M \sum_{n=-N}^N h_{m,n} a_{l-m,k-n} + n_{l,k}, \quad (1)$$

where  $h_{m,n}$  is the coefficient of a discrete 2-D channel response,  $m$  and  $n$  represent the indices of the bit islands in the along-track direction and the across-track direction, and  $n_{l,k}$  is an additive white Gaussian noise (AWGN). The coefficients of the discrete channel response,  $h_{m,n}$ 's are normally generated by sampling the isolated island's pulse response at the integer multiples of the bit period  $T_x$  and the track pitch  $T_z$ , i.e.,

$$h_{m,n} = A \exp \left\{ -\frac{1}{2} \left[ \left( \frac{anT_x}{PW_x} \right)^2 + \left( \frac{bmT_z}{PW_z} \right)^2 \right] \right\}, \quad (2)$$

where  $A$  is the peak amplitude of the pulse response,  $PW_x$  and  $PW_z$  are the widths of the pulse response at its half maximum ( $PW50$ ), and the notation  $a$  and  $b$  are the fitting parameters related to the head/media geometry. In this study, both  $a$  and  $b$  are set to  $2\sqrt{2\ln(2)}$ . In the readback channel model, we assumed that three readback signal sequences  $\{r_{-1,k}\}$ ,  $\{r_{0,k}\}$  and  $\{r_{1,k}\}$  from the tracks  $l \in \{-1, 0, 1\}$  are received at the input of data recovery system. In the system, a 2-D equalizer  $\mathbf{F}$  equalizes the readback signal sequence  $\{r_{0,k}\}$  from the main track  $l = 0$  according to the 2-D GPR target  $\mathbf{G}$  with the help of sidetrack sequences,  $\{r_{-1,k}\}$  and  $\{r_{1,k}\}$ . The equalized signal sequence,  $\{z_{0,k}\}$  is then processed by a Viterbi detector embedded with noise predictor. Both equalizer  $\mathbf{F}$  and GPR

target  $\mathbf{G}$  are simultaneously designed by a minimum mean squared error (MMSE) technique which minimizes the mean squared error (MSE) between the equalized signal sequence  $\{z_{0,k}\}$  and the desired output sequence  $\{d_{0,k}\}$  which is the output of the target.

## III. VITERBI DETECTOR WITH NOISE PREDICTOR

In the data recovery system, the equalized signal sample  $z_{0,k}$  can be expressed as

$$z_{0,k} = \sum_{i=-1}^1 \sum_{j=-L}^L f_{i,j} y_{-i,k-j} + \sum_{i=-1}^1 \sum_{j=-L}^L f_{i,j} n_{-i,k-j}, \quad (3)$$

where  $y_{l,k}$  is the noiseless channel output signal sample and  $f_{i,j}$  is the coefficient of 2-D equalizer  $\mathbf{F}$ . According to the second term in (3), the equalizer will correlate the additive noise of the received signals, and then the resulted noise becomes the colored noise that degrades the performance of Viterbi detector. However, this performance inferiority can be alleviated by integrating a noise predictor into the detector. In the noise predictor, the noise sample  $\omega_{0,k}$  is defined as the difference or error sample between the equalized readback signal sample,  $z_{0,k}$  and the desired output sample,  $d_{0,k}$ , i.e.

$$\omega_{0,k} = z_{0,k} - d_{0,k}, \quad (4)$$

where  $d_{0,k} = \sum_{m_g} \sum_{n_g} g_{m,n} a_{-m,k-n}$  is computed with the coefficients  $g_{m,n}$ 's of the GPR target  $\mathbf{G}$  with size  $M_g \times N_g$ . It is important to notice that the noise sample  $\omega_{0,k}$  in (4) includes not only a correlated noise but also the residual interference due to mis-equalization. Since the noise sample is correlated with the neighboring samples due to the equalizer, the current noise sample can be predicted based on the past noise samples [6].

### A. Noise Prediction Filter

In a linear predictor model, the predicted current noise sample can be defined as,

$$\hat{\omega}_{0,k} = \sum_{i=1}^K p_i \omega_{0,k-i}, \quad (5)$$

where  $\omega_{0,k-i}$  is a previous noise sample at time delay  $i$  from (4),  $p_i$  is the coefficient of the linear noise prediction FIR filter  $P(D)$ , and  $K$  is the length of the filter. To design the filter, the mean squared error (MSE) of the noise prediction error is defined as

$$E \left[ \|\omega_{0,k} - \hat{\omega}_{0,k}\|^2 \right] = E \left[ \left\| \omega_{0,k} - \sum_{i=1}^K p_i \omega_{0,k-i} \right\|^2 \right]. \quad (6)$$

The optimal coefficients of prediction filter  $p_i$  can be found by minimizing the mean squared error in (6). Let  $\mathbf{p} = [p_1, p_2, \dots, p_K]^T$  be a column vector of the coefficients of the noise prediction filter and then it can be expressed

$$\mathbf{p} = \mathbf{R}_{\omega\omega}^{-1} \mathbf{r}_{\omega}, \quad (7)$$

where  $\mathbf{r}_{\omega\omega} = E[\omega_{0,k}\omega]$  and  $\mathbf{R}_{\omega\omega} = E[\omega\omega^T]$  are an auto-correlation vector and an autocorrelation matrix of the noise samples sequence  $\omega = [\omega_{0,k-1}, \dots, \omega_{0,k-K}]^T$  respectively.

Alternatively, the noise sample can be predicted using an IIR filter. The IIR filter can provide the performance improvement without increasing the number of filter taps. Therefore, we also consider the IIR filter for noise prediction in this study. For IIR noise prediction, the predicted noise sample is written as a recursive equation, i.e.,

$$\hat{\omega}_{0,k} = \sum_{j=1}^K (\alpha_j + \beta_j) \omega_{0,k-j} - \sum_{j=1}^K \alpha_j \hat{\omega}_{0,k-j}, \quad (8)$$

where  $\alpha_j$  and  $\beta_j$  are the zero-pole parameters of the IIR filter and  $K$  is the length of the filter. The zero-pole parameters in (8) can be calculated from the autocorrelation function of noise sample sequence as described in [7].

### B. Proposed Noise Prediction

With the predicted noise sample, the branch metric of the Viterbi detector for a state transition at time  $k$  is modified as,

$$\lambda(S_{k-1}^m, S_k^n) = [z_{0,k} - d_k(S_{k-1}^m, S_k^n) - \hat{\omega}_{0,k}]^2, \quad (9)$$

where  $S_{k-1}^m$  and  $S_k^n$  are the previous  $m^{\text{th}}$  state and the current  $n^{\text{th}}$  state at time  $k$  for  $m, n \in \{1, 2, \dots, M_s\}$ ,  $d_k(S_{k-1}^m, S_k^n)$  is the target output sample generated with the input bits of the branch and the bits defined in the state  $S_{k-1}^m$ , and  $M_s$  is the total number of states in the trellis. Based on (5) and (8), the predicted noise sample  $\hat{\omega}_{0,k}$  is computed with the previous noise samples,  $\omega_{0,k-i}$ 's for  $i \in \{1, \dots, K\}$ , and the previous noise sample computation consequently requires a number of past input bits from three tracks, but they are beyond the input bits of the state  $S_{k-1}^m$  of the given trellis. Therefore, in the conventional technique, the trellis is redesigned based on the effective target  $G_f(D) = G(D)[1 - P(D)]$  to attain the previous noise samples, and the noise whitening filter,  $[1 - P(D)]$  is added before the detector. However, this technique is not appropriate for the Viterbi detector of the 2-D interference channel because of the high complexity.

In this work, we propose to use a technique that stores the past noise samples along the surviving path leading to the current state for the noise prediction so that it doesn't need to extend the trellis. In particular, the Viterbi algorithm computes  $\omega_{0,k}$  which is the difference between the equalized signal sample  $z_{0,k}$  and the desired output sample  $d_k(S_{k-1}^m, S_k^n)$  of the state transition for the branch metric computation at time  $k$ . In the proposed technique, this computed  $\omega_{0,k}$  is stored as the noise sample associated to that  $S_k^n$  state, i.e.  $\omega(S_k^n)$  for the future noise prediction if the respective branch is selected as a part of the surviving path. Since the surviving path include the sequence of most likely past states leading to the current state, those noise sample are most reliable information to predict the current noise. For the branch metric calculation at each transition, it is assumed that the prediction algorithm can access the stored information along the surviving path in depth of the length of the predictor. With the previous noise

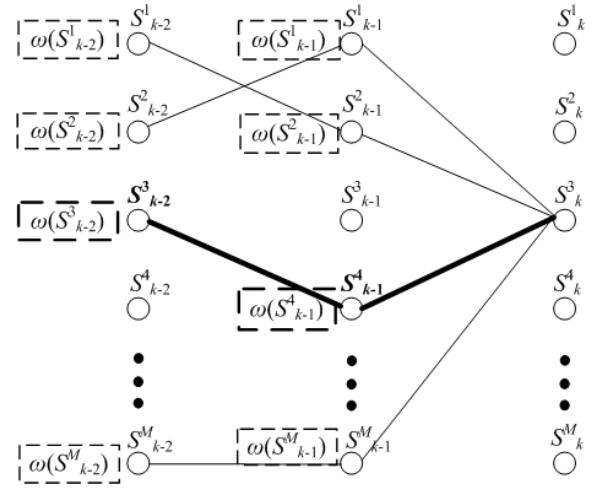


Fig. 2. The hypothetical surviving paths with stored noise samples for the proposed noise prediction technique.

samples stored along the surviving path leading to the current state  $S_k^n$ , the branch metric equation in (9) is rewritten as

$$\lambda(S_{k-1}^m, S_k^n) = \left[ z_{0,k} - d_k(S_{k-1}^m, S_k^n) - \sum_{i=1}^K p_i \omega(S_{k-i}^m) \right]^2. \quad (10)$$

For an example of a Viterbi detector the noise predictor of length  $K = 2$ , the system will read back two previous stages along the surviving path. The trellis with the hypothetical paths that stores the noise samples for this example is demonstrated in Fig. 2. When the branch metric of the transition from the previous state  $S_{k-1}^4$  to the current state  $S_k^3$  at time  $k$  is computed, the predicted noise sample is estimated with the previous noise samples along the surviving path leading the current state through the previous state (the bold lines in Fig. 2), i.e.,  $\omega(S_{k-1}^4)$  from the time  $k-1$ , and  $\omega(S_{k-2}^3)$  from the time  $k-2$ . For other branch metric calculations, the current noise samples are predicted with the past noise samples along their respective surviving paths. Finally, the current noise sample  $\omega(S_k^3) = z_{0,k} - d_k(S_{k-1}^4, S_k^3)$  is stored at the state  $S_k^3$  for further noise prediction if that branch is selected as a part of surviving path. Since the information along the surviving path are the most reliable, it is expected that the predicted noise sample based on them are also most reliable and enhance the performance of Viterbi detector.

The proposed noise prediction technique needs one extra storage for each state, and  $K$  more multiplications and additions for predicting the noise sample at each branch metric computation than the detector without noise predictor. As a result, the complexity increment of the proposed noise prediction technique is significantly less than the noise prediction by extending the trellis in [7]. However, this noise prediction technique needs a precaution for error propagation because the past noise samples are computed with the tentative estimates of input bits based on the most likelihood or surviving path.

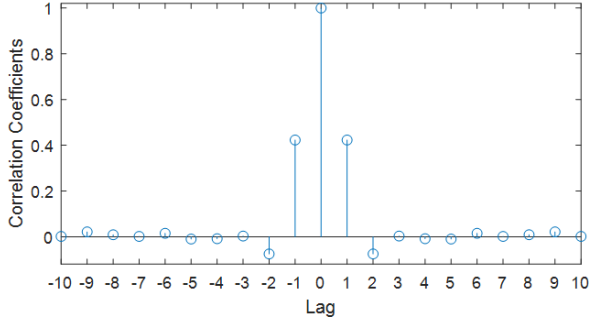


Fig. 3. The autocorrelation of the noise sample  $\omega_{0,k}$ .

#### IV. SIMULATION RESULT AND DISCUSSION

In this work, we consider the BPMR systems of two high areal densities, 3 Tbits/in<sup>2</sup> and 4 Tbits/in<sup>2</sup> by setting the respective pairs of bit period and track pitch. The along-track  $PW50$  and across-track  $PW50$  are considered with 19.4 nm and 24.8 nm respectively and each data sequences sector contains 4096 bits. The signal-to-noise ratio (SNR) is defined as  $20\log_{10}(V_p/\sigma_k)$  where  $V_p = 1$  is the peak value of the readback signal and  $\sigma_k$  is the standard deviation of AWGN. The 2-D target  $\mathbf{G}$  with size of 3x3 and the 2-D equalizer  $\mathbf{F}$  with 3x11 are designed with the BPMR channel at the SNR level 22 dB. The 2-D channel response matrices with the size of 5x3 generated by (2) at the areal densities 3 Tbits/in<sup>2</sup> and 4 Tbits/in<sup>2</sup> are

$$\mathbf{H}_3 = \begin{bmatrix} 0.004 & 0.021 & 0.004 \\ 0.078 & 0.379 & 0.078 \\ 0.205 & 1 & 0.205 \\ 0.078 & 0.379 & 0.078 \\ 0.004 & 0.021 & 0.004 \end{bmatrix}, \quad (11)$$

$$\mathbf{H}_4 = \begin{bmatrix} 0.017 & 0.055 & 0.017 \\ 0.147 & 0.483 & 0.147 \\ 0.305 & 1 & 0.305 \\ 0.147 & 0.483 & 0.147 \\ 0.017 & 0.055 & 0.017 \end{bmatrix}. \quad (12)$$

Firstly we study the autocorrelation function of the noise samples sequence  $\{\omega_{0,k}\}$  in (4) for the BPMR readback channel model. The autocorrelation function of the samples sequence of the BPMR channel at 4 Tbit/in<sup>2</sup> is shown in Fig. 3. It is obviously that the noise sample sequence is correlated, and the non-zero coefficients at first lag are the most significant and other coefficients are not as obvious as the coefficients of the first lags. Therefore, we employ the FIR noise predictor with only one tap and the IIR noise predictor with single-pole to avoid the error propagation problem. The coefficients of FIR noise prediction filter are computed with the autocorrelation functions of errors samples using (7) and the coefficients of IIR filter are computed like [7] using a known training sequence.

The bit error rate (BER) performances of the Viterbi detectors embedded with the proposed prediction technique are compared to that of the detectors without noise predictor

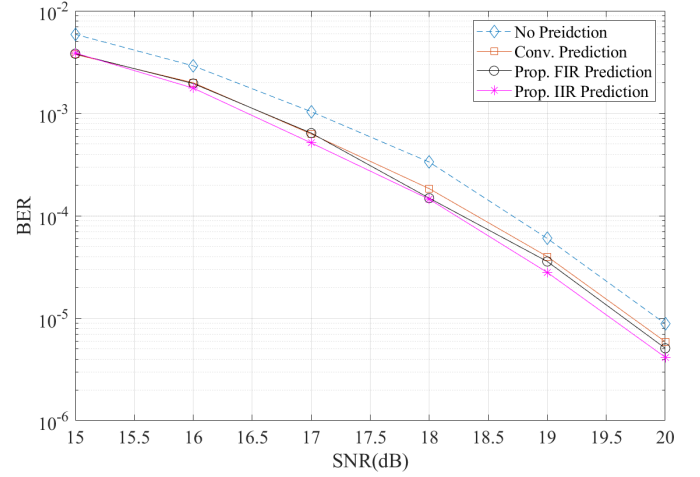


Fig. 4. Performance of the Viterbi detectors with and without various noise prediction techniques for BPMR system with 3 Tbit/in<sup>2</sup>.

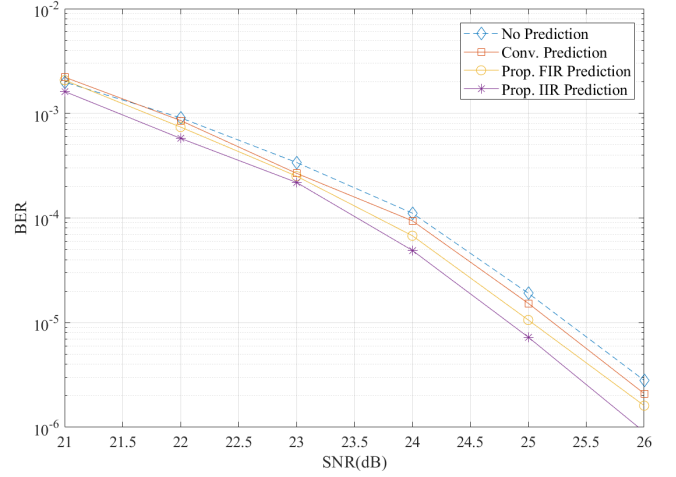


Fig. 5. Performance of the Viterbi detectors with and without various noise prediction techniques for BPMR system with 4 Tbit/in<sup>2</sup>.

and with the conventional noise predictor that employs a extended trellis. The performance of detectors for the BPMR system of 3 Tbits/in<sup>2</sup> is shown in Fig. 4. All detectors with noise predictor provide better performance than the detector without noise predictor. The performance of the proposed noise predictor with FIR filter is not significant from that of conventional predictor, although the IIR predictor provides the best performance gain. At the areal density in 4 Tbits/in<sup>2</sup>, the proposed noise predictions performs significantly better than others as depicted in Fig.5. The predictor with IIR filter achieves the performance gain about 0.5 dB and the predictor with FIR about 0.4 dB over the detector with no noise predictor. In both areal densities, the noise prediction technique with extending trellis is inferior to the proposed techniques in the 2-D interference channel of BPMR system.



## V. CONCLUSION

In this paper, we study the performance of two Viterbi detectors with noise predictor for the 2-D interference channel of high areal density BPMR system. To avoid the high complexity, we propose a noise detection technique in which the current noise sample is estimated using the past noise sample sequence that stored along the surviving path. For noise prediction filter, we consider one filter tap for FIR filter and a single-pole fir IIR filter to minimize the error propagation. The simulation results show that the detectors with proposed noise techniques can provide the performance gain over the detector without noise predictor and with the noise prediction by extending the trellis.

## ACKNOWLEDGMENT

This work was supported by the office of the Higher Education Commission Thailand and the Thailand Research Fund (TRF) under grant MRG6080110.

## REFERENCES

- [1] P. W. Nutter, I. T. Ntokas, and B. K. Middleton, "An investigation of the effects of media characteristics on read channel performance for patterned media storage," *IEEE Trans. Magn.*, vol. 41, no. 11, pp. 4327-4334, Nov. 2005.
- [2] S. Nabavi and B. V. K. V. Kumar, "Two-dimensional generalized partial response equalizer for bit-patterned media," in *Proc. ICC 2007, Glasgow, Scotland, 2007*, pp. 6249-6254.
- [3] S. Karakulak, P. H. Siegel, J. K. Wolf and H. N. Bertram, "Joint-track equalization and detection for bit patterned media recording," *IEEE Trans. Magn.*, vol. 46, no. 9, pp. 3639-3647, Sept. 2010
- [4] W. Chang and J. R. Cruz, "Inter-track interference mitigation for bit-patterned magnetic recording," *IEEE Trans. Magn.*, vol. 46, no. 11, pp. 3899-3908, Nov. 2010.
- [5] G. Forney, "Maximum-likelihood sequence estimation of digital sequences in the presence of intersymbol interference," *IEEE Trans. Inf. Theory*, vol. 18, no. 3, pp. 363-378, May 1972.
- [6] P. R. Chevillat, E. Eleftheriou, and D. Maiwald, "Noise-predictive partial-response equalizers and applications," in *Proceedings of ICC*, pp. 942-947, IEEE, 1992.
- [7] J. D. Coker, E. Eleftheriou, R. L. Galbraith, and W. Hirt, "Noise-predictive maximum likelihood (npml) detection," *IEEE Trans. Magn.*, vol. 34, no. 1, pp. 110-117, 1998.
- [8] J. Caroselli, S. A. Altekari, P. McEwen and J. K. Wolf, "Improved detection for magnetic recording systems with media noise," *IEEE Trans. Magn.*, vol. 33, no. 5, pp. 2779-2781, Sept. 1997.
- [9] J. Moon and J. Park, "Pattern-dependent noise prediction in signal-dependent noise," *IEEE J. Select. Areas on Commn.*, vol. 19, no. 4, pp. 730-743, 2001.
- [10] E. Chesnutt, "Novel turbo equalization methods for the magnetic recording channel," Ph.D dissertation, Georgia Institute of Technology 2005.
- [11] M. N. Kaynak, T. M. Duman and E. M. Kurtas, "Noise predictive belief propagation," in *IEEE Trans. Magn.*, vol. 41, no. 12, pp. 4427-4434, Dec. 2005.